General Disclaimer

One or more of the Following Statements may affect this Document

- This document has been reproduced from the best copy furnished by the organizational source. It is being released in the interest of making available as much information as possible.

- This document may contain data, which exceeds the sheet parameters. It was furnished in this condition by the organizational source and is the best copy available.

- This document may contain tone-on-tone or color graphs, charts and/or pictures, which have been reproduced in black and white.

- This document is paginated as submitted by the original source.

- Portions of this document are not fully legible due to the historical nature of some of the material. However, it is the best reproduction available from the original submission.

NASA CONTRACTOR REPORT

NASA CR-141430

CALIBRATION RESULTS FOR THE GEOS-3 ALTIMETER

C.F. Martin
M.L. Butler

Prepared Under Contract No. NAS6-2639 by

EG&G/Washington Analytical Services Center, Inc.
Wolf Research and Development Group
6801 Kenilworth Avenue
Riverdale, Maryland 20840

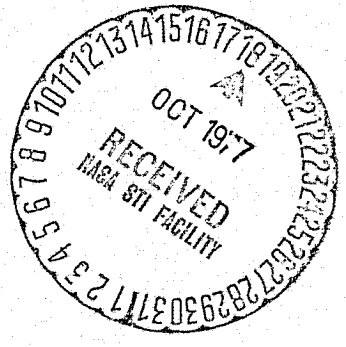

National Aeronautics and
Space Administration

Wallops Flight Center
Wallops Island, Virginia 23337
AC 804 824-3411

September 1977

1. Report No.	2. Government Accession No.	3. Recipient's Catalog No.
NASA CR-141430		

4. Title and Subtitle	5. Report Date
Calibration Results for the GEOS-3 Altimeter	September 1977
	6. Performing Organization Code

7. Author(s)	8. Performing Organization Report No.
C.F. Martin; M.L. Butler	
	10. Work Unit No.

9. Performing Organization Name and Address	11. Contract or Grant No.
EG&G/Washington Analytical Services Center, Inc. Wolf Research & Development Group 6801 Kenilworth Avenue Riverdale, MD 20840	NAS6-2639
	13. Type of Report and Period Covered
12. Sponsoring Agency Name and Address	Contractor Report
National Aeronautics and Space Administration Wallops Flight Center Wallops Island, VA 23337	14. Sponsoring Agency Code

15. Supplementary Notes

16. Abstract

Data from the GEOS-3 altimeter was analyzed, for both the intensive and global modes, to determine the altitude bias levels for each mode and to verify the accuracy of the time tags which have been applied to the data. The best estimates of the biases are:

Intensive Mode	-5.30 m $\pm$ .2 m
Global Mode	-3.55 m $\pm$ .4 m

These values include the approximately 1.6 m offset of the altimeter antenna focal point from the GEOS-3 spacecraft center-of-mass. The negative signs indicate that the measured altitudes are too short. The data is corrected by subtracting the above bias numbers for the respective modes.

The adopted intensive mode bias is based on a GEOS-3 pass through the calibration, across the island of Bermuda, on February 25, 1976 at approximately 3 P.M. local time. This pass was tracked by NASA lasers at Grand Turk, Bermuda, and Goddard, and its groundtrack passed 32 m Southwest of the Bermuda laser site in a South-North direction. The direction was across the narrow dimension of the island and land was in the altitude measurements for less than 1.5 seconds. The calibration method used for this pass involved an orbit determined by the 3 laser tracking stations, smoothed altimeter data across Bermuda with the land data deleted, and a tidal correction based on tide gauges at Bermuda. This technique effectively produces an altimeter measurement for the spacecraft directly over the tracking stations, thus avoiding any influence of geoid model error on the result.

The global mode bias was estimated through comparisons (overlaps and crossovers) of global mode passes and intensive mode passes through the calibration area. An off-nadir correction was made for each pass, and the bias estimated is for a nadir looking altimeter.

Timing corrections which should be applied to the altimeter data were calculated theoretically, and subsequently confirmed through crossover analysis for passes 6-8 revolutions apart. The time tag correction that should be applied consists of

-20.8 msec + 1 interpulse period (10.240512 msec).

17. Key Words (Suggested by Author(s))	18. Distribution Statement
calibration GEOS-3 altimeter	Unclassified - unlimited STAR category 19

19. Security Classif. (of this report)	20. Security Classif. (of this page)	21. No. of Pages	22. Price*
Unclassified	Unclassified	123	

*For sale by the National Technical Information Service, Springfield, Virginia 22151

ACKNOWLEDGEMENTS

The authors would like to express their appreciation for the assistance of a number of people who have contributed in various ways to the analyses included in this report. The large number of private communications included in the references attests to some of these individuals. In addition to those explicitly referenced, thanks are due the GEOS-3 Project Scientist, H. Ray Stanley, for a number of helpful discussions as well as a critical review of the draft report, and to Dr. John Zarur of WASC who made a major contribution to the timing analysis given in Appendix A.

TABLE OF CONTENTS

TABLE OF CONTENTS
(Cont.)

LIST OF FIGURES

LIST OF FIGURES

(Cont.)

LIST OF TABLES

LIST OF TABLES

(Cont.)

SECTION 1.0
INTRODUCTION

The GEOS-3 spacecraft, launched on April 9, 1975, began operational activities on April 21, 1975. Since that time, the GEOS-3 altimeter has taken data on several thousand passes. On most of these the altimeter was operating in the more precise short pulse, or intensive, mode. However, several hundred long pulse, global mode passes of data have been taken.

In order for the altimeter data to fulfill its goal in the determination of a global geoid, it is necessary that the GEOS-3 altitude data be corrected so that it gives correct measurements of the distance from the spacecraft center-of-mass to the instantaneous mean sea surface height at the sub-satellite point. This requires that any bias between the measured and true altitudes be determined so that the data can be appropriately used in absolute geoid determination. Two such estimates of both global and intensive mode altimeter biases have been made. The first estimates, based on pre-launch measurements on the actual GEOS-3 flight model altimeter by G.E. [1], gave center-of-mass bias values of (negative biases mean measurements are short):

Intensive Mode	-	-6.55 m
Global Mode	-	-0.68 m

The second set of bias estimates was made by Martin and Butler [2], based on analysis of 19 passes of in-flight data taken during the first operational month. Biases estimated were:

Intensive Mode	-	-0.79 m
Global Mode	-	+0.11 m

The latter study also concluded that, based on the consistency of intensive mode bias estimates from North-South and South-North passes, the accuracy of altimeter data time tags for data processed at Wallops Flight Center was approximately 20 msec or better.

The above agreement between the two global mode biases appears satisfactory enough, but the intensive mode bias disagreement suggests that something may be systematically wrong with one calibration or the other. In addition to these agreements and disagreements, two other items added to the uncertainty in the altimeter calibration:

- Calibrations of the first month's (and other) data using a different, more detailed, geoid model* gave bias numbers some 3 meters smaller than the above in-flight numbers for both intensive and global modes.

- In approximately mid 1976, it was discovered and verified [4] that the NASA STDN timing for GEOS-3 contained a 20.8 msec bias. Altimeter data analyses did not appear to indicate a timing error of this magnitude.

In addition to these disturbing and confusing developments, several other developments took place which, together, allowed a resolution of most of the uncertainties. Among these were:

- A number of altimeter passes through the GEOS-3 calibration area occurred with supporting ground

*The earlier calibrations were performed using a 15' x 15' geoid [3]. The later calibrations used one or more versions of a 5' x 5' geoid.

tracking from the NASA lasers at Bermuda, Grand Turk, and Greenbelt, Maryland (GSFC). After appropriate relative station adjustment, this allowed the estimation of very precise laser orbits.

- Several intensive mode altimeter passes over Bermuda took place, including one which was tracked by the Bermuda, Grand Turk, and GSFC lasers. The latter pass was almost overhead at the Bermuda laser.

- A data smoother was developed for GEOS-3 altimeter data. The smoother allows smoothing across bad or deleted data points and was used to smooth data across Bermuda with the land data deleted, resulting in an effective altimeter measurement to mean sea level at the tracking site. In addition, the smoother allows very precise comparisons of altimeter measurements at crossovers.

The bias calibrations presented in this report make extensive use of orbits determined by lasers when available, and by C-Band radars at Wallops Island and Bermuda when 3 laser tracking is not available. In the case of global mode calibrations, only one pass was supported by 3 laser tracking, and C-Band support was thus essential. With the exception of some of the intensive mode calibrations using extended data segments and the geoid model as a reference, all calibrations used the altimeter data smoother.

The calibration results presented in Section 3 for the intensive mode appear to be consistent, to within expected accuracies, both between different in-flight calibrations and with current interpretations of pre-launch altimeter calibration data. Global mode calibration results appear to be consistent between different passes, although they are not consistent with

the pre-launch calibration data. Timing errors are treated somewhat differently than the altitude biases. An analytical derivation of the appropriate time tag for altitude data is given in Appendix A, and a correction computed which should be applied to the time tags of altimeter data processed at Wallops Flight Center. This correction is applied in both the intensive and global mode calibrations. Consistency of altimeter crossovers for passes ~12 hours apart is then used to verify that the time tags are correct. The crossover tests using smoothed data should be sufficiently sensitive to detect timing errors of more than 2-3 msec, provided temporal sea surface height variations are negligible between passes. In fact they are not always negligible, but the overall crossover analysis is consistent with the processed data being time tagged correctly.

The recommended biases which should be applied to global and intensive mode altimeter data are summarized in Section 5.

SECTION 2.0
CALIBRATION METHOD

In general, the calibration of the GEOS-3 altitude measurements requires the computation of the measurement that the altimeter should be making and comparing it with the observed altitude measurement. Any discrepancy is then attributed to a net uncompensated system bias. The implementation of this procedure is most readily accomplished in terms of heights above a reference ellipsoid. The satellite height above the ellipsoid is determined through the use of ground tracking data, and the sea surface height above the ellipsoid is determined through one of several different procedures. In all cases, we consider the sea surface height above the reference ellipsoid to be composed predominantly of a stationary geoid height and a time varying tidal height. Three different procedures have been utilized for the computation of geoid heights for use in the GEOS-3 altimeter data analysis. These are:

1. The use of a geoid model based upon gravimetric data taken in the calibration area.

2. Geoid height estimation by the altimeter data itself on the same pass.

3. Geoid height estimations made by the GEOS-3 altimeter on other passes.

In all cases, a tide model is necessary to account for temporal variations of sea surface height. Quasi-stationary departures of the sea surface from the stationary geoid + periodic tides are neglected in the sense that no corrections are made for them. They are, however, believed to be observed, and will be discussed in connection with intensive mode calibration in Section 3.

Calibration procedures involving the three different techniques for accounting for geoid heights are discussed below in Sections 2.1 - 2.3. The geoid and tide models utilized are then discussed in Sections 2.4 and 2.5, respectively. Two of the calibration techniques require that the altimeter data be smoothed, so that the comparison of sea surface heights can be made as accurately as possible at altimeter crossovers. The technique used for data smoothing is discussed briefly in Section 2.6. Finally, it should be noted that the GEOS-3 altimeter global mode is significantly affected by off-nadir pointing errors. An attempt is made to correct for such effects based on certain characteristics of the altimeter return pulse shape. The remaining difference between measured and calculated global mode altitudes will then hopefully be a constant, and is then the desired bias calibration. The off-nadir correction technique is discussed in Section 2.7.

2.1 CALIBRATION BASED ON GEOID MODEL

The original method planned, and used, for GEOS-3 altimeter calibration is simple enough in concept. The essential elements are:

1. The orbit is calculated with the best available set of well calibrated tracking stations, and using only a single pass of data ($\lesssim$ 10 minutes) so that geopotential model error is essentially zero.

2. A pass of altimeter data, typically several minutes long, is used in the portion of the pass where the orbit is considered to be best determined.

3. The altimeter measurement is calculated, accounting for

   a. The height of the geoid above the ellipsoid based upon a geoid model.

   b. The tide height above the geoid based upon a tide model.

4. The tracking station heights are rectified to the geoid model by computing their ellipsoid height as the sum of mean sea level and geoid heights. Mean sea level heights are obtained from local surveys and geoid heights are obtained from the geoid model.

Assuming unbiased trackers, good station coordinates, and good geoid and tide models, this method is capable of a high degree of accuracy. Because several minutes of data are used, the effects of measurement noise are, for all practical purposes, negligible.

The area chosen as the GEOS-3 calibration area was basically the quadrangle formed by ground tracking stations at Wallops Island, Bermuda, Grand Turk, and Merritt Island. Original calibration plans called for C-Band radars and Doppler Geoceivers at each of these sites and for S-Band radars at Bermuda and Merritt Island. These instruments were to be supplemented by mobile lasers at Bermuda and Grand Turk and by permanent laser installations at Wallops Island and Merritt Island (actually, Patrick AFB). In addition to these four primary sites, tracking stations at Antigua (C-Band radar), Goddard Space Flight Center (laser and S-Band) and Rosman (S-Band) were potentially available for improving the satellite orbits. Instruments which turned out to be available and which have produced data most useful for calibration purposes were:

- NASA Mobile Laser at Bermuda
- NASA Mobile Laser at Grand Turk
- NASA Stationary Laser at GSFC
- Two NASA C-Band Radars at Wallops Island
- NASA C-Band Radar at Bermuda

The mathematical model used for this altimeter calibration mode is based on the geometry shown in Figure 1. The altimeter makes a series of measurements to the instantaneous electronic mean sea level (IEMSL) while passing between a set of ground stations which are tracking GEOS-3 simultaneously. Based on data from the ground tracking stations, the satellite height above the reference ellipsoid, h_{el}, can be estimated. From the geometry of Figure 1, h_{el} has a number of components which can be broken down as

$$h_{el} = h_{alt-b} + h_{geoid} + h_{tide} + \delta h \qquad (1)$$

where

h_{alt} = the actual altimeter measurement corrected for propagation effects (noise is neglected here), but not bias.

b = altimeter bias.

h_{geoid} = the height of the geoid at the subsatellite point above a reference ellipsoid.

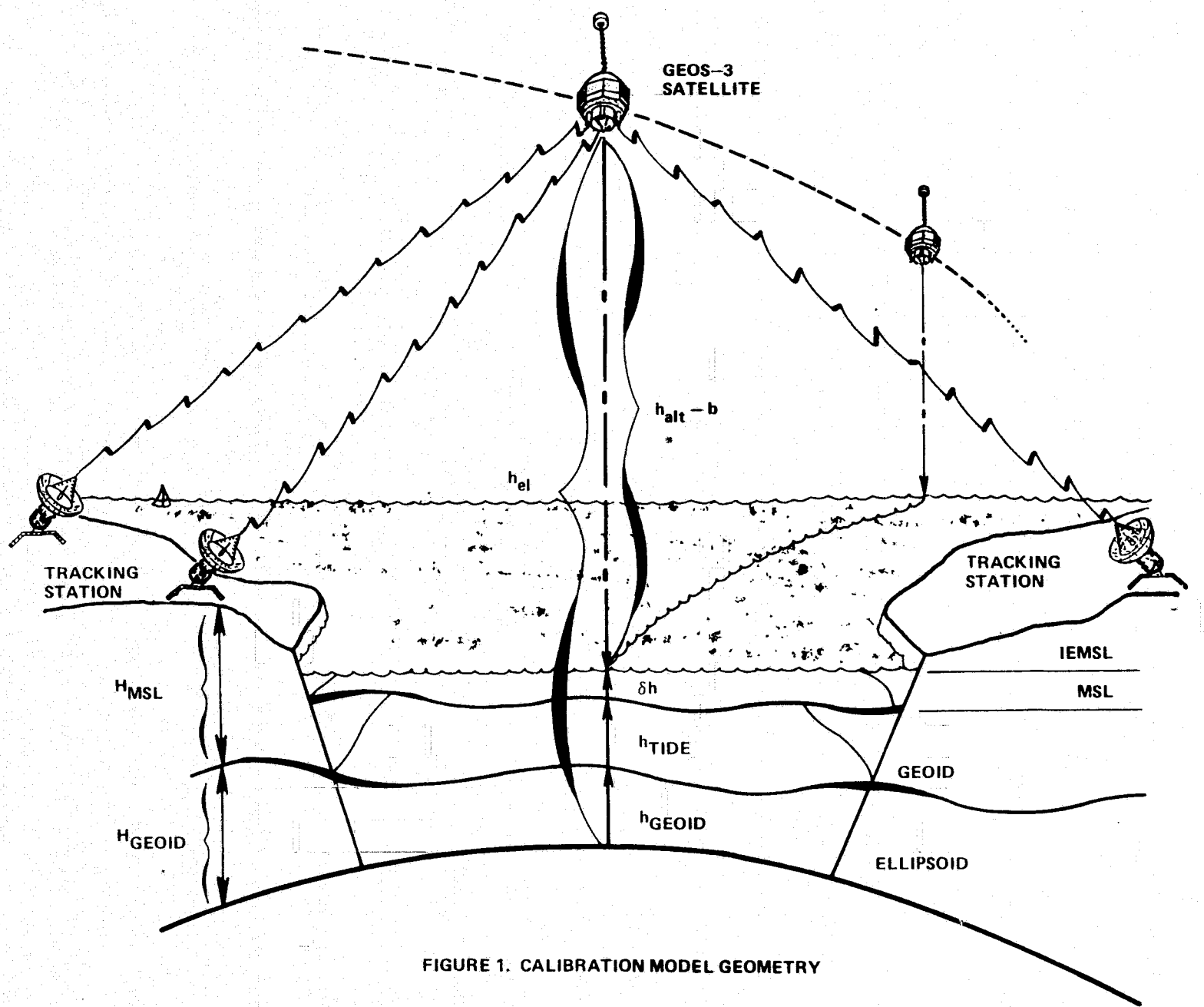

FIGURE 1. CALIBRATION MODEL GEOMETRY

h_{tide} = the height of the ocean tide above the local geoid at the subsatellite point.

δh = the instantaneous deviation of the actual instantaneous mean sea surface from the mean sea level height after tidal corrections. This term includes such effects as currents, eddies, any deviation of the true mean sea surface from the "electronic" mean sea surface (i.e., effects of waves), etc.

In the actual calibrations, the term δh is neglected since most of the time it will be small (~10 cm) and, in any event, there is no reliable procedure for calculating it. The Gulf Stream is on the western edge of the calibration area, and can have sea surface height effects on the order of a meter at its boundaries. However, altimeter data for the Gulf Stream region is generally not used in the calibrations. Height effects greater than 50 cm can also exist for cold water eddies which do exist in the calibration area, particularly in the northern portion. When these occur, we simply live with their effects. But if they occur rather infrequently and/or over limited regions, their effects will be minimized since this calibration technique averages effects over a number of passes, each of which is several minutes long. It may be noted, however, that the effects of eddies on the calibration bias would be expected to be systematic, producing a bias which is too large algebraically, since the sea surface height over the cold water eddies will be abnormally low and the resulting altimeter measurements abnormally long.

The GEODYN program [5] at WFC was used for the simultaneous estimation of the altimeter bias and the satellite orbit for a single pass through the calibration area. The estimation algorithm used was such that, although both altimeter and ground tracking data were weighted in the solution, only the ground tracking data was used in the orbit estimation. When

C-Band radar data was used in these calibration solutions, biases were always fixed, having been separately determined in previous one or two revolution orbital solutions.

It should be noted that the accuracy of this calibration method is highly dependent upon the accuracy of the geoid model available. And the most significant factor here is the accuracy with which the model is tied to the island tracking stations. Since geoid variations in the vicinity of islands are almost always quite high, it is not surprising that the tie of an island to the at sea geoid should be particularly difficult.

To a lesser degree, station position errors in latitude and longitude are also a significant source of error in the calibrations which do not involve a pass near a tracking station. This problem, however, is considered to have been satisfactorily solved for the laser tracking stations. See Appendix B.

2.2 HIGH ELEVATION CALIBRATION

The geometry for the pass of the satellite directly over a tracking station is shown in Figure 2. This figure also shows the components of the calculation of the ellipsoid to satellite measurement based upon both the orbit and upon the altimeter measurement. Equating these two,

$$h_{alt} - b + \delta h + h_{tide} + h_{geoid}\ (Alt)$$

$$= R + h_{MSL} + h_{geoid}\ (Sta) \qquad (2)$$

= Height of orbit above ellipsoid

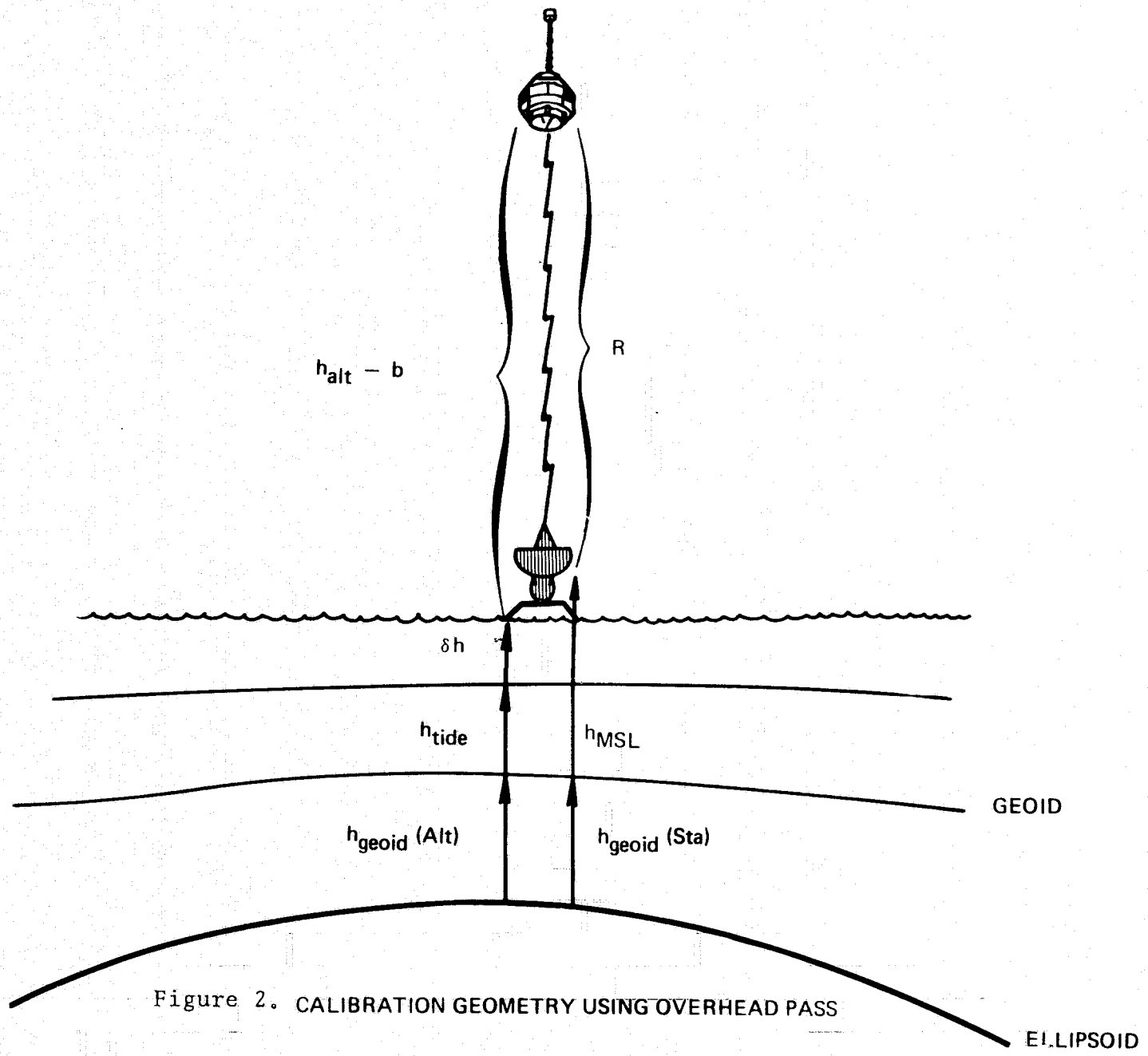

Figure 2. CALIBRATION GEOMETRY USING OVERHEAD PASS

Solving for the altimeter bias, and noting the source of the measurements required in the bias computation, we obtain

Measurement	Source
$b = h_{alt} - R$	Measurements from satellite pass
$- h_{MSL}$	Local survey
$+ h_{tide}$	Tide model or tide gauges (3)
$+ [h_{geoid}\ (Alt) - h_{geoid}\ (Sta)]$	Geoid model
$+ \delta h$	Non-geoidal, non-tidal variations - assumed negligible

This relation differs in two important respects from the bias determined through the use of Eqn. (1). In the first place, the most important error source in the use of Eqn. (1) was the geoid model error. In Eqn. (3), any such errors cancel. Secondly, the tide model may not necessarily be expected to be valid for the overhead calibration. This means that, in order to use the overhead calibration method, an alternative means of determining sea surface height above mean sea level may be required. Tide gauges, suitably located, are an acceptable substitute.

In principle, then, the overhead calibration method is really very simple, and the use of such a technique involving a laser tracker on a ship at sea was one of the original calibration proposals for GEOS-3. It was never proposed for a land tracker because of the infrequency of overhead passes and the perturbing influence of land in the footprint. The fact that it can be used for GEOS-3 must be considered quite fortuitous in that:

- A pass occurred so nearly overhead at the Bermuda laser tracking site.

- The direction of the pass was across the narrow dimension of Bermuda so that land was in the footprint for less than 1.5 sec.

- The pass was supported by both laser and radar tracking at Bermuda, as well as by lasers at Grand Turk and GSFC.

Only one such pass has occurred during the lifetime of GEOS-3. Altimeter data was scheduled for this pass and the ground stations all supported. The a priori probability of all these events was certainly not very high.

Even with the altimeter data across Bermuda, passing directly over the tracking station, it is not immediately obvious how the calibration could be accurately performed without the use of an accurate geoid model in the vicinity of Bermuda. This subject will be discussed in more detail in Section 3.2 when the actual data reduction is considered for the overhead pass.

2.3 CALIBRATION BASED ON COMPARISON WITH CALIBRATED PASSES

This method is both simple and self explanatory. In practice, the GEOS-3 intensive mode was calibrated first and was found to be reasonably stable. In the process a number of precise orbits were obtained. Consequently, it was decided to base the global mode calibrations on cross-over differences with the good intensive mode passes. The primary problem lay in choosing the portion of the pass to make the comparisons, since the global mode orbits were generally not as accurate as

those for the intensive mode passes* due to a lesser amount of supporting ground tracking. This choice could normally be made on the basis of ORAN [6] analysis of the propagation of measurement biases and station position errors into orbital height errors. In general, this area was in the northern portion of the calibration area.

In addition to the intersections of the global mode passes with intensive mode passes, there were several cases in which global mode passes essentially overlapped intensive mode passes. In such cases, a graphical matchup of altimeter residuals along a several minute orbital segment was considered superior to the intersection differences. Smoothed residuals were always used in these comparisons.

2.4 GEOID MODEL

All altimeter data reductions for the GEOS-3 calibration effort have used the Marsh-Chang 5' x 5' geoid model [7] for the calibration area between the latitude bands of 16°N to 39°N, and between the longitude bands of 278°E to 300°E. In all cases, the use of the model facilitated data smoothing and the identification of significant orbit error trends. For the first calibration method, requiring the correlation of mean sea level at the tracking sites with mean sea level at sea, the geoid is critical and systematic errors in it can be expected to be passed on into the estimated altimeter biases.

---

*Because of the much larger number of intensive mode passes, it was possible to be very selective in requiring 3 laser tracking and still obtain a reasonable number of passes. The same criterion applied to the global mode passes would have resulted in only one pass. Consequently, tracking requirements were relaxed to require only two stations with good geometry relative to the pass.

In order to rectify the tracking stations being used [2] to the Marsh-Chang geoid, the following shifts in height were required:

Goddard	+ 2.78 m
Grand Turk	+ 2.64 m
Wallops Island	+ 2.78 m
Bermuda	+ 5.67 m

As is evident, there is a tilt of about 3 m about a SE axis between Bermuda and the other stations. Based on a large number of station height estimations by various people, it appears that some of the tilt is in the station positions and some is in the geoid model. In any event, it is not a source of great concern, since the rectification process is supposed to eliminate a large percentage of the effects of a tilt in the geoid model. The tie of the geoid model to the island tracking stations is of considerably more concern, and errors here do indeed introduce systematic errors into recovered biases.

2.5 TIDE MODEL

Ocean tides appear to have amplitudes on the order of half a meter, and it is necessary to account for such effects in order to make calibrations at the sub-meter accuracy level. The model which has been used for all altimeter calibrations is an empirical model obtained by Mofjeld [8] specifically for GEOS-3 calibration purposes. The approximate boundaries of applicability of the model are 27°-35°N latitude and 285°-295°E longitude as shown in Figure 3. Within this region, the model is specified by Mofjeld to have an accuracy of $\pm$5 cm. The degradation of the model outside the region indicated in Figure 3, particularly in the north-east direction,

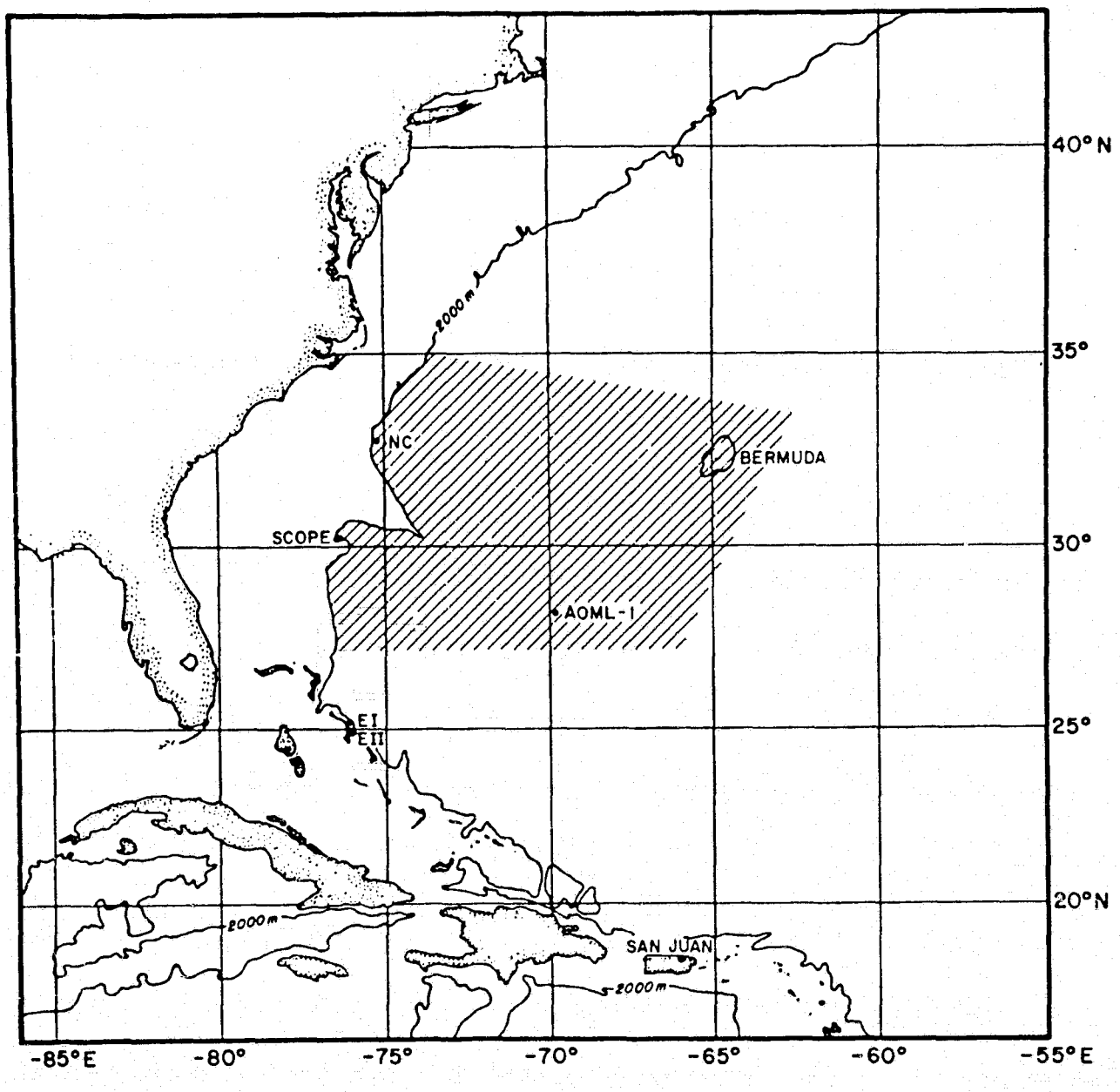

FIGURE 3. GEOS-3 CALIBRATION AREA IN THE WESTERN ATLANTIC WITH REFERENCE AND TEST STATIONS AND THE GEOGRAPHICAL EXTENT OF THE GEOS-3 TIDE MODEL AS DEFINED BY THE CROSS-HATCHED REGION REPRODUCED FROM MOFJELD [8]

is not considered to be very rapid, and some calibrations were performed outside the proper area for which the tide model was derived. Resulting contributions to altimeter calibration uncertainties are not considered to be very serious.

2.6 OFF-NADIR MODEL

The GEOS-3 altimeter global mode, due to its long pulse width, can be significantly affected by the antenna not pointing exactly along the nadir direction. Although the spacecraft is considered to be stabilized to within a degree of nadir better than 90% of the time, off-nadir angles greater than 0.5° still produce effects which should be taken into account in both the instrument evaluation and the use of the data.

The GEOS-3 spacecraft instrumentation includes both a digital solar sensor and a magnetometer for use in determining spacecraft attitude. This instrumentation was intended, however, primarily for use in spacecraft capture and its use for definitive attitude has produced results estimated to be accurate to ~0.5°. [9].

A potentially somewhat more accurate approach has been proposed by Applied Science Associates [10,11]. In this approach, measured altimeter return pulse characteristics are averaged over some period of time and then used to estimate the off-nadir angle. The off-nadir angle can then be transformed into a global mode altitude bias [12] relative to the altitude that would have been measured had the altimeter antenna been pointed towards nadir. The effective bias as a function of off-nadir angle is shown in Figure 4.

FIGURE 4.

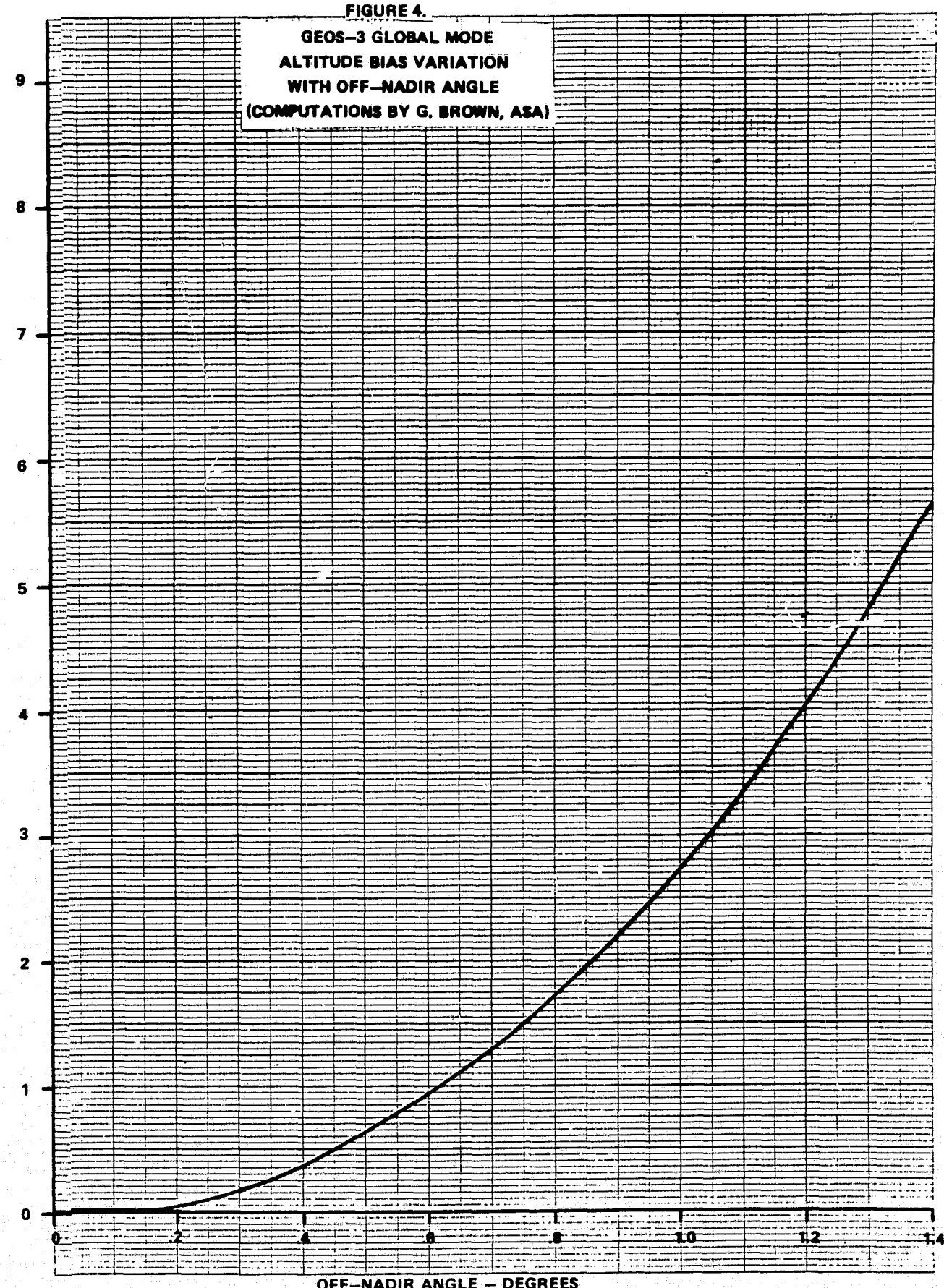
GEOS–3 GLOBAL MODE
ALTITUDE BIAS VARIATION
WITH OFF–NADIR ANGLE
(COMPUTATIONS BY G. BROWN, ASA)
9
8
7
6
5
4
3
2
1
0
0
.2
.4
.6
.8
1.0
1.2
1.4
OFF–NADIR ANGLE – DEGREES

Both the ASA algorithm for off-nadir angle computation and the corresponding bias given by Figure 4 are programmed in the Wallops GEODYN program and global mode calibrations are automatically referenced to a "nadir" looking altimeter. To the extent that the resulting biases are consistent for different computed off-nadir angles, it really does not matter whether the computed off-nadir angle is correct or not. The interpretation can be made that the altimeter return pulse is distorted, and the "off-nadir" correction then properly accounts for the effects on measured altitude. Making this correction and the constant bias correction then produce the proper satellite to sea surface measurement.

It should be noted that the altimeter intensive mode is also affected by off-nadir viewing angles, although the magnitude of the effects has been estimated to be only at the few centimeter level [13]. If these estimates are indeed valid, off-nadir effects are negligible compared to other known error sources.

2.7 DATA SMOOTHING

The a priori noise levels expected for GEOS-3 cumulative altitudes (i.e., data at the 10 pps rate) are approximately

- 60 cm for intensive mode
- 1 m for global mode.

A number of methods have been proposed for smoothing altitude data so that it can be used at less than the 10 pps rate without losing any significant information. The simplest scheme proposed, and the easiest one (by far) to implement, is to perform a linear fit in time to the altitude data over a major frame (~2 or 3.2 seconds). The smoothed altitude on the GEOS-3 altimeter data tapes is computed in this manner, and probably

represents near optimum smoothing so long as each frame of data is handled separately. As a smoothing technique, however, the procedure has some severe limitations. The most important limitations are:

1. The smoothing operation should involve data over a time period longer than a major frame. This conclusions has been reached in an analytical study [14], based on the optimum estimation of geoidal heights in the presence of nominal noise levels and geoidal undulations. Based on the expected wavelengths and amplitudes of non-geoidal undulations such as those due to current boundaries, the conclusion is believed to be valid for all sea surface heights estimated from GEOS-3 data.

2. Extrapolation from periods of "good" data to periods of bad or nonexistent data is virtually impossible.

3. Identification of bad data points is difficult, particularly when a significant portion of a major frame is bad.

Limitation No. 2 would not normally be considered a serious problem for global geoid production, since a procedure for extrapolation or interpolation would have to be incorporated anyway. For one of the calibration techniques, however, interpolation between good data points is required to as high degree of accuracy as possible.

A solution to the above data smoothing/interpolation problems has been implemented in the ALTKAL [15] program, developed explicitly for the smoothing of GEOS-3 altimeter data. The basic elements of this program are:

1. A Kalman filter, operating on cumulative altitude data, nominally available at ~10 pps, with a state

model based upon random noise errors in the altimeter measurements and a third order Markov model for geoid undulation features. Missing data points can be simply skipped across and bad data points can be deleted using rather tight edit criteria.

2. A Kalman filter operating on the data exactly as in 1, except that it starts at the end of a data pass and proceeds backward in time.

3. An optimum combination of the forward and backward filter results to produce optimum estimates of both heights and slopes.

For altimeter calibration purposes, ALTKAL was operated with the input of GEODYN output residuals, with orbit, tides and the Marsh-Chang 5' x 5' geoid already removed. In plots of ALTKAL output, no high frequency noise is evident*, and altimeter crossover comparisons are thus greatly facilitated. However, the most useful feature of the program is its ability to accurately smooth across missing (or deleted) data points in the presence of rapid geoid undulations. Without such a capability, the overhead calibration technique could not have been applied.

*Noise on the data does propagate as low frequency effects, with the amplitude and frequency dependent upon the filter parameters. See Section 3.2.1.

SECTION 3.0
INTENSIVE MODE CALIBRATION

The primary objectives in the calibration of altitudes from the GEOS-3 altimeter intensive mode have been to:

1. Determine the true measurement bias which can be used to correct the data, producing a measurement from the spacecraft center-of-mass to the instantaneous mean sea level at the subsatellite point.

2. Determine the stability of this bias.

3. Determine the existence of any time tag errors in the data.

It is believed that these objectives have all been met to a level that is consistent with the accuracy of the data itself, and the results are given below in Sections 3.1 and 3.2. In the calibration process, however, certain other problems arose whose explanation or solution are significant if maximum accuracy is to be achieved in the utilization of the data. These problems include:

1. Apparent anomalies, occurring irregularly, in which the altitude measurements are long by on the order of 4-6 m for periods of ~0.5 second.

2. Altitude bias variation as a function of TM mode.

These problems are also discussed in this section. It is believed that at least a phenomenological explanation of the anomalies is available, so that the proper handling of them can be made. The differences between biases for different TM modes appears to be satisfactorily resolved on the basis of the data itself, although other analyses have predicted conflicting results.

3.1 BIAS DETERMINATION

Two different methods have been used for the estimation of the GEOS-3 altimeter intensive mode bias. The first method has been used for 16 different passes through the calibration area. Results from these calibrations will be described first. Next, we consider the single sample of the overhead type calibration. An assessment of the accuracy achieved will be made in Section 3.5 after the consistency of different passes at their intersections has been examined in Section 3.2.

3.1.1 Bias Determination Using Geoid Model

The technique used for bias estimation based on a geoid model has been described in Section 2.1. Initially, it was planned that all altimeter passes through the calibration area with sufficient ground tracking for the estimation of a good orbit would be processed for altimeter bias estimation. In some cases, this requirement extended to the existence of tracking on adjacent revolutions in order that radar calibrations could be performed. However, the altimeter calibration was always performed using ground tracking data from only a single pass through the calibration area.

The Marsh-Chang 5' x 5' geoid model [7], transformed to a 6378145 m ellipsoid, was used as the reference geoid, with the resulting set of bias estimates shown in Table 1. Groundtracks for these passes, showing the approximate segment of altimeter data used, are shown in Figure 5. Also included in Table 1 is the set of tracking stations used to determine the orbit for each calibration pass.

It will be noted from Table 1 that the pass to pass bias estimations have a 1σ spread of less than 30 cm about a

TABLE 1. INTENSIVE MODE BIAS ESTIMATIONS USING RADAR/LASER ORBITS AND MARSH–CHANG 5′ x 5′ GEOID MODEL

REV NO.	DIRECTION	ESTIMATED BIAS	TRACKING STATIONS USED*
203	S–N	– 4.10 m	WAL/BDR/BDL/GRT
246	S–N	– 4.80 m	WAL/BDR/STA/GRT
524	N–S	– 4.46 m	WAL/BDR/GRT
530	S–N	– 3.99 m	WAL/BDR/GRT
1107	N–S	– 4.60 m	WAL/BDL/GRT
1312	S–N	– 4.76 m	WAL/GRT
1710	S–N	– 4.32 m	STA/BDL/GRT
1966	S–N	– 3.92 m	WAL/STA/GRT
1974	N–S	– 4.56 m	STA/BDL/GRT
2017	N–S	– 4.00 m	STA/GRT
2037	S–N	– 3.98 m	BDA/GRT
2094	S–N	– 4.48 m	STA/BDL/GRT
2102	N–S	– 4.44 m	STA/BDL/GRT
2108	S–N	– 4.22 m	WAL/STA/BDL
2165	S–N	– 4.45 m	STA/GRT
2244	N–S	– 4.23 m	WAL/BDL/GRT
	AVERAGE	– 4.33 m ± .27 m (1σ SCATTER)	

* WAL – NASA FPQ–6 or FPS–16 C–Band Radar at Wallops Island
BDR – NASA FPQ–6 C–Band Radar at Bermuda
STA – NASA Staionary Laser at GSFC
BDL – NASA Mobile Laser at Bermuda
GRT – NASA Mobile Laser at Grand Turk

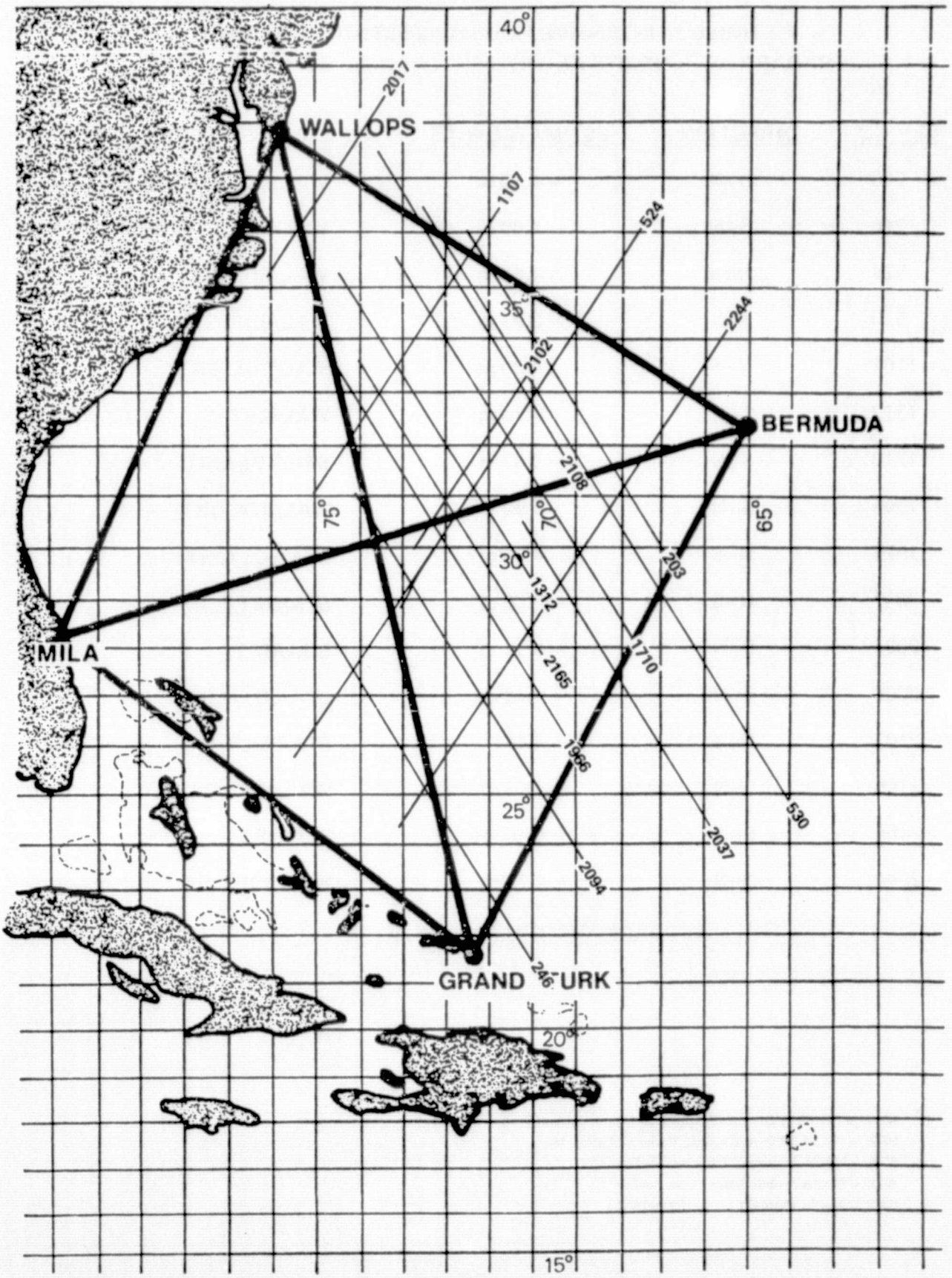

FIGURE 5. GROUND TRACKS FOR INTENSIVE MODE CALIBRATIONS USING GEOID MODEL IN SEA SURFACE HEIGHT COMPUTATIONS

mean bias of -4.3 m. Based on this apparently consistent bias recovery, passes other than these 16 were not processed for bias estimation using the geoid model technique. Instead, attention was concentrated on identifying the possible existence of systematic errors in all passes. The analyses discussed below in Section 3.1.2 were the result.

It might be noted that several of the passes listed in Table 1 have 3 laser tracking, and that these passes are very consistent (total spread - 16 cm). Their mean is also very close to the overall mean. This might be interpreted to mean that the laser only orbits give a more accurate result. Because of the small sample size and the known problems with geoid rectification, we prefer to attach little significance to this consistency, although it is definitely to be expected that the 3 station orbits would be more accurate than the 2 station orbits.

No set of error components has been formally prepared for the results shown in Table 1. In order of importance, these are considered to be geoid rectification errors and horizontal station position errors, with all other error sources on the order of 10 cm or less. The geoid and station position errors would be expected to have both systematic and random components from one pass to the next, due to the varying geometry from pass to pass. These error sources could easily account for the observed scatter in estimated biases although, at this stage, pass to pass variation by the altimeter has not been ruled out. The systematic component of the geoid and station position errors is difficult to estimate without reliable covariances for the geoid model error. These, in turn, are difficult to obtain. However, systematic effects on the order of 1-2 m are probably in the right ballpark. Given the nature of historical geoid model changes, it might be expected that the geoid height of Bermuda (the most important

station) would be underestimated relative to the surrounding ocean areas, and so the resulting bias estimates would be more likely to be too large (algebraically) than to be too small. Comparisons with the bias value estimated by G.E. [1] from the analysis of altimeter system delays would tend to support this contention.

3.1.2 Bias Calibration Using Rev 4553

Several altimeter passes have passed sufficiently close to Bermuda to have land in the footprint. Groundtracks of several of these passes are shown in Figure 6. However, only Rev 4553 was supported by ground tracking from Bermuda. Laser data taken by the three NASA lasers on this pass is listed in Table 2. The data from several of the other passes across Bermuda have been processed, including smoothing, and their measurement of the geoid in the vicinity of Bermuda are consistent with Rev 4553. Since these other passes have no tracking tie to Bermuda, we will not make use of them in the calibration discussion, although they could be used in a redetermination of the appropriate rectification of the current calibration area geoid.

A plot of the altimeter residuals after orbit estimation is shown in Figure 7. These residuals are the measured cumulative altitudes minus the computed orbit height above the ellipsoid, with corrections made for tropospheric propagation, tides, and the Marsh-Chang 5' x 5' geoid. The laser tracking station position used, however, had a height above ellipsoid of -25.90 m, consistent with the "best" set of station positions discussed in Appendix B. Considering the mean sea level height of 13.45 m, this is equivalent to using a geoid height of -39.35 m, whereas the geoid model height at the laser site is -33.69 m. There is thus a discrepancy of

ORIGINAL PAGE IS
OF POOR QUALITY

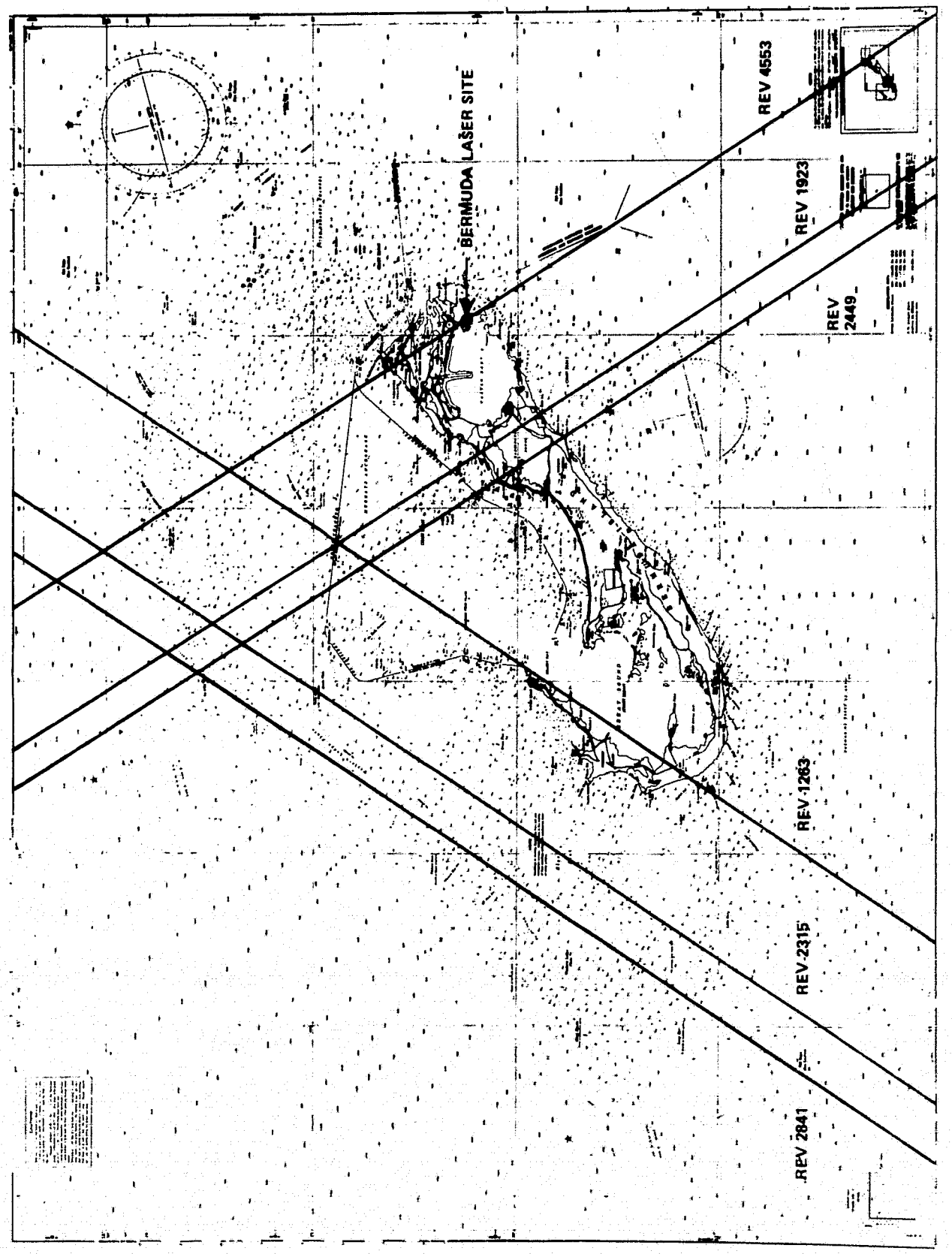

FIGURE 6. GROUND TRACKS OF ALTIMETER PASSES ACROSS BERMUDA

Station	Start of Track		End of Track		Max. El.	Total No. of Points	No. of Wtd.Pts.	RMS of Wtd.Pts.
	Time	Elevation	Time	Elevation				
Grand Turk	$19^h12^m06^s$	23°	$19^h16^m07^s$	20°	28°	146	145	4.96 cm
Bermuda*	$19^h13^m04^s$	37°	$19^h15^m51^s$	74°	74°	33	30	5.21 cm
	$19^h\ 16^m\ 54^s$	48°	$19^h17^m02^s$	46°	46°	3	3	3.80 cm
Goddard	$19^h18^m17^s$	58°	$19^h18^m24^s$	58°	58°	2	2	.81 cm
Totals						184	180	4.96 cm

*Data segments before and after ~1 minute data gap are summarized separately.

Table 2. Laser Tracking Support on GEOS-3 Rev 4553, February 25, 1976.

FIGURE 7. ALTIMETER RESIDUALS ACROSS BERMUDA ON GEOS-3 REV 4553
MARSH 5' x 5' GEOID REMOVED

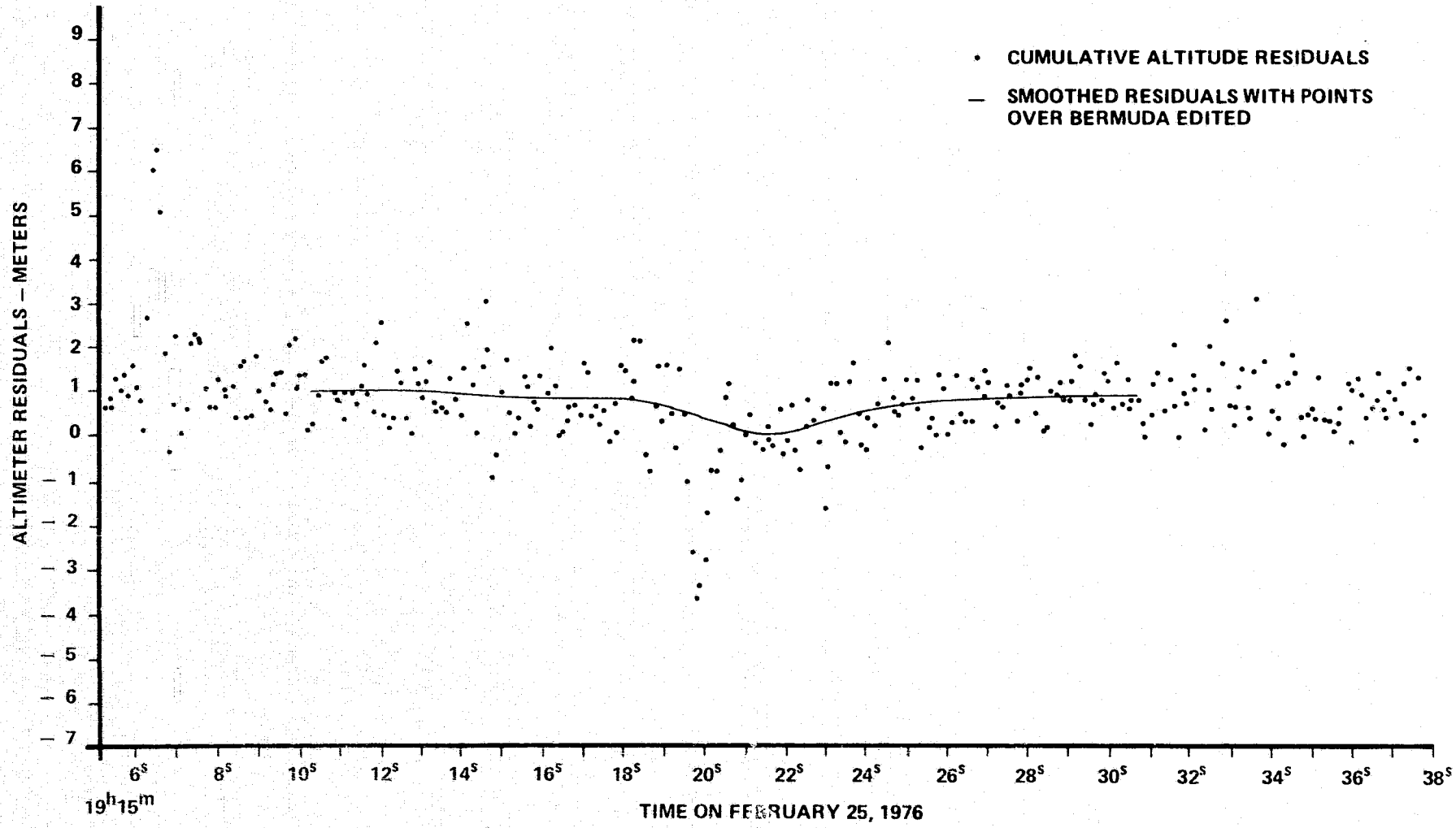

5.66 m between the geoid height used in computing the orbit and the geoid height used in computing the geoid correction to the altimeter measurement. But there should not be any orbit error induced over Bermuda because of station rectification to fit the geoid. This factor is of considerable significance for this pass because, as shown in Table 2, Bermuda did not track continuously on this pass and indeed did not track through maximum elevation.

Figure 7 also shows the smoothed residuals across Bermuda, after zero-weighting points which would have Bermuda in the footprint, based on the nominal footprint diameter of 3.5 km. Assuming minimal error from the smoothing operation and that the tide model is valid across Bermuda, the altimeter residuals as smoothed across Bermuda represent the Marsh-Chang geoid minus the geoid as measured by the altimeter. Figure 7 then says that the geoid model underestimates the geoid height of Bermuda relative to adjacent deep sea areas by something on the order of a meter. This suggests that the bias estimates given in the previous section in Table 1 would indeed be systematically large, algebraically, as we have previously speculated.

Before proceeding further, we must dispose of the two assumptions required in order to interpret the smooth curve in Figure 7 as representing error in the geoid model:

1. Tide Model Validity

   The tide model is not, according to Mofjeld [8], valid within ocean depths of 2000 m or less. There was, however, a tide gauge [16] along the 4553 ground track and its measurements were consistent with the tide model predictions to within approximately 7 cm. Tidal corrections are discussed in Appendix C.

2. Smoothing Validity

The ALTKAL smoother is based upon geoid undulation and altimeter noise models which have no requirement for continuous data. When data points are deleted or not weighted, the uncertainty in the estimated height goes up. Within the limits of this expanded variance, there is no reason for the smoothed residuals across Bermuda not to represent local geoid model error. The smoothed height sigma across Bermuda reaches approximately 17 cm, compared to an ~12 cm sigma with no data deletions, based upon nominal noise and geoid model parameters.

We can now proceed to an expanded view of the smoothed residuals across Bermuda as shown in Figure 8. Here the deleted data segment is explicitly shown, as is the time of closest passage of the spacecraft ground tracks to the Bermuda laser. The time of this passage is $19^h\ 15^m\ 19^s.6272$ UTC time on February 25, 1976. The subsatellite track passes about 32 m SW of the laser site. From the ALTKAL run, the altimeter residual at this time is 0.533 m.

Table 3 summarizes the components of the bias computation based on the altimeter "measurement" crossing the Bermuda laser tracking site. The data reduction was performed using measured meteorological data from Bermuda for making tropospheric refraction corrections for the altimeter data. However, an ionospheric propagation correction is needed since the local time is just prior to 3 P.M. This correction has been estimated using ORAN [6] to be about 10 cm. Since the tide model correction is estimated in Appendix C, the only other needed components of the bias computation are the "observed" residual and the separation in geoid heights at the laser site between the geoid model and that corresponding to the station position used in the data reduction. The net result is a bias estimate of -5.3 m for the intensive mode bias.

FIGURE 8. ALTIMETER RESIDUALS ACROSS BERMUDA ON GEOS-3 REV 4553
MARSH–CHANG 5′ x 5′ GEOID MODEL REMOVED

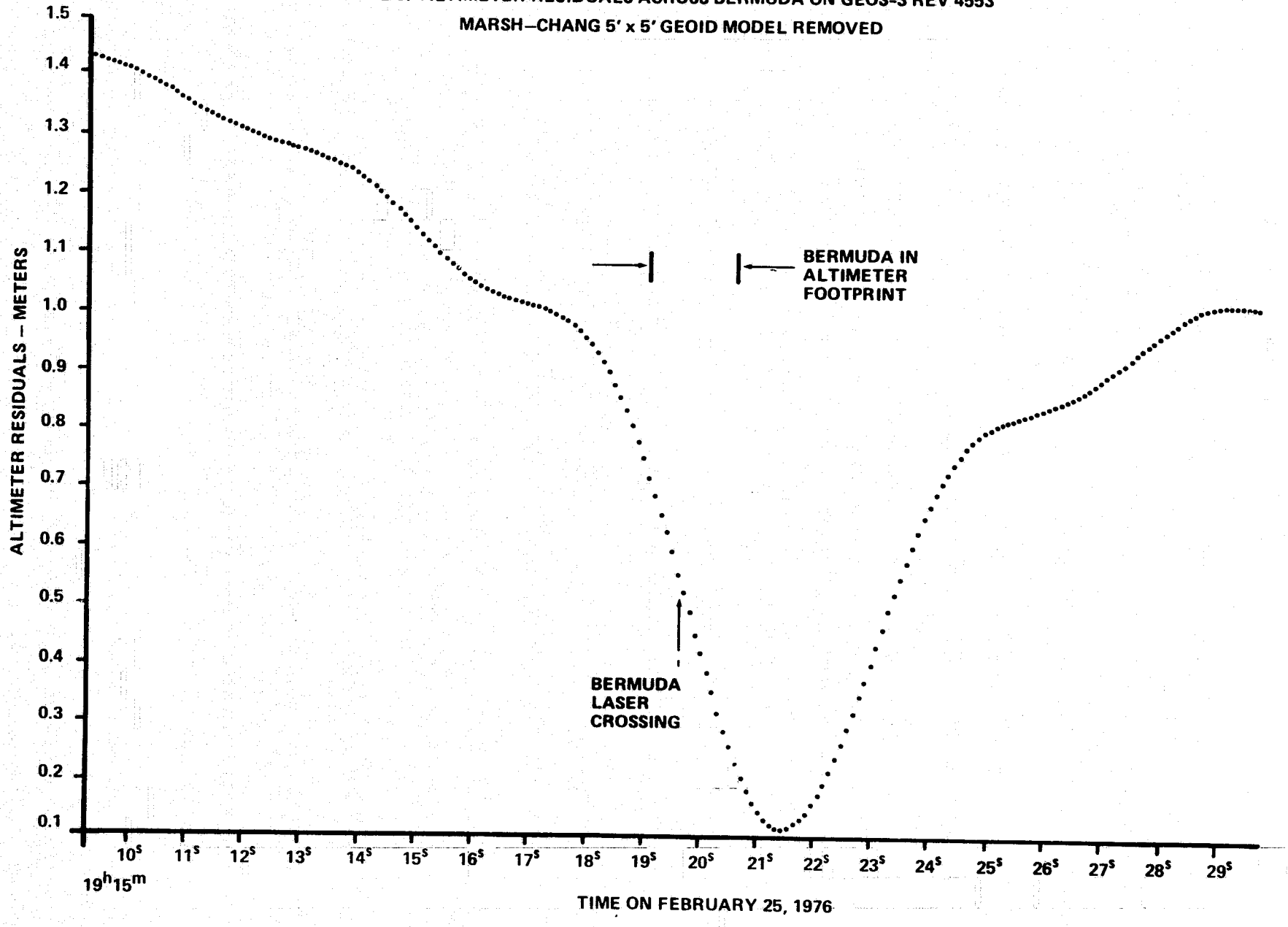

Component	Value
Measurement residual	0.53 m
+ Geoid height used for tracking station - Geoid height used for altimeter measurement computation	-5.66 m
+ Ionospheric propagation correction	-.10 m
+ Tide Model correction (Appendix C)	-.07 m
Bias	-5.30 m

Table 3. Computation of Intensive Mode Bias From Overhead Calibration on Rev 4553

Although the geoid model has been used throughout this section, it cancels out completely in the final bias computation. It should be noted, however, that the elimination of this error source is not without a price. And this price has already been alluded to as an increase in the uncertainty in the altimeter geoid height during periods of no data, or no good data. This increased uncertainty, however, is believed to be substantially less than the systematic errors in the geoid model, even though such local errors may be only on the order of a meter.

3.2 CONSISTENCY OF INTENSIVE MODE ALTITUDE DATA

There are three reasons for considering the consistency of the GEOS-3 altimeter data:

1. To ascertain any variability of the altitude bias, either short term or long term. Particularly is this of interest since we have obtained our presumably most accurate bias estimate on the basis of a single pass.

2. To look for evidence of any remaining timing errors on the altitude time tags.

3. To investigate the accuracy with which the altimeter is capable of mapping short wavelength sea surface features. An in depth answer to this question is beyond the scope of this report, but certain aspects must be considered in the interpretation of altimeter measurements at points at which different passes "cross over" the same geographic sub-satellite point.

In this section, we will consider the available evidence for bias stability and valid time tags. The altimeter's measurement of short wavelength undulations will be considered as necessary in this evaluation.

As the primary basis for this analysis, we consider the set of 18 calibration area passes* which were tracked by the three NASA lasers located at Bermuda, Grand Turk, and GSFC. As discussed in Appendix B, station positions were estimated specifically for use in obtaining consistent orbits for this set of passes. It is believed that the baselines associated with this set of station positions have accuracies on the order of 10-20 cm. The heights, however, may be considerably less accurate, even relative to each other. If there were continuous laser tracking by all stations during the altimeter pass through the calibration area, trilateration positioning could be used around each crossover, and none of the station position errors would be significant. However, there appear to be NO crossovers for which trilateration positioning can be done for both orbits, and we have thus resorted to the estimation of a single best orbit for each pass. The difference in the orbit height errors at crossover points depends upon the tracking data available for the two passes, as well as the station baseline and height errors. The difference errors will thus vary from one crossover to the next. For a "typical" crossover, however, we estimate that this error may be on the order of 25-30 cm, but probably are normally much less. A tracking data problem could cause a larger effect, but no evidence of such exists.

Figure 9 shows the agreement of the 18 passes at their crossover points. The crossover differences have a mean of

*This set of 18 is complete for tracking by 3 NASA lasers on a calibration area pass with altimeter data taken with operation in the intensive mode. Use of the RML laser data increases the number of 3 laser passes, some of which will be considered below.

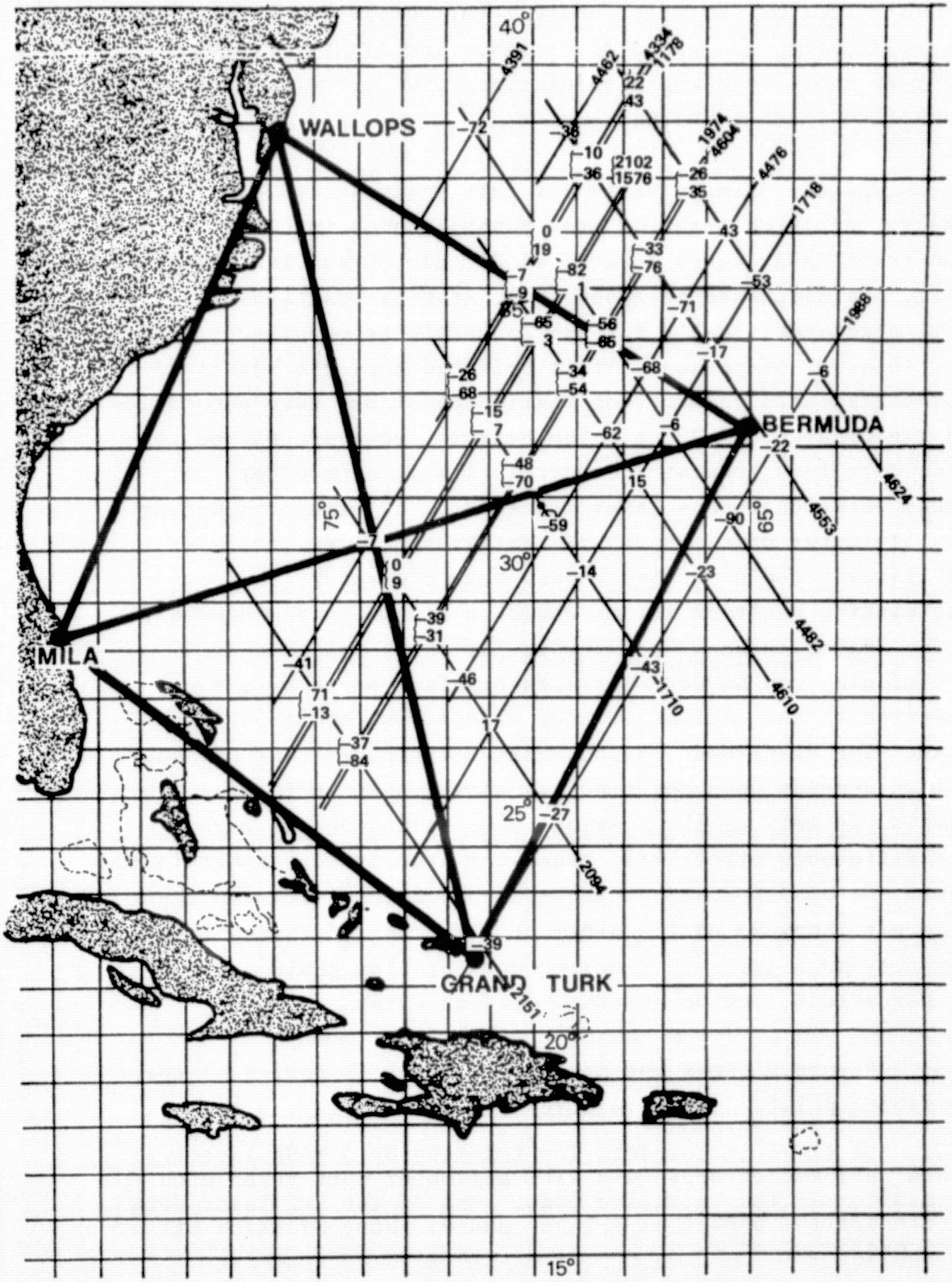

FIGURE 9. ALTIMETER CROSS–OVER DIFFERENCES FOR INTENSIVE MODE PASSES HAVING 3 LASER TRACKING. SIGN CONVENTION IS N–S MEASUREMENT – S–N MEASUREMENT

-30 cm, with a one standard deviation scatter about this mean of 36 cm. So the non-zero value of the mean is only on the borderline of being significant. On the assumptions that there are no pass to pass bias variations and no altimeter time tag errors, the explanation for the crossover differences must lie in some combination of the following four error sources:

a. Orbit error. Regardless of the source (expected to be predominantly station position errors), the effect should be very nearly linear along each pass.

b. Altimeter noise. The data has been smoothed prior to computing the crossover differences. However, the 1σ effect on the residual is still on the order of 12 cm, which will be independent from one pass to the next and, in most cases, from one intersection to the next.

c. Propagation effects. Only Revs 4553 and 1988 have been corrected for tropospheric propagation effects based on measured meteorlogical data, and even here only for the conditions at the time of Bermuda passage. In other cases, a constant correction has been applied which, in general, underestimates the correction. The maximum undercorrection is estimated to be on the order of 10 cm. No ionospheric correction has been made for any pass, with the maximum effect estimated at about 10 cm for daytime passes.

d. Temporal sea surface variations. Much of the GEOS-3 calibration area is very "smooth" in the sense of having only very long wavelength geoidal features.

However, the area does contain currents and eddies. The 4 northernmost intersections in Figure 9 lie north of the nominal western boundary of the Gulf Stream. Eddies from the Gulf Stream move south, and the entire area north of approximately the latitude of Bermuda would be likely candidates for an eddy being present on one pass and not on another. No part of the calibration area would be considered totally immune from eddies.

It will be noted from Figure 9 that there are three pairs of nearly overlapping tracks from the set of passes tracked by the 3 NASA lasers. These passes have been used to attempt to determine the magnitude of temporal sea surface height variations. Figures 10-12 show measurement residuals from these 3 pairs of passes. No attempt has been made to realign the plots to compensate for orbit errors, either in bias or slope. When no evidence of bias or slope exists, then the differences must be interpreted either as measurement error (due to noise effects) or to temporal sea surface variations. The existence of apparent within-pass variations of 1 m or more indicates that a significant portion of the differences shown in Figure 9 may be attributable to temporal changes in sea surface height.

Two sets of overlaps have also been examined for which the RML laser provides the third laser for one of the tracks. Residuals for these overlaps are shown in Figures 13 and 14. In both cases, RML tracked on the same pass as the Bermuda and Grand Turk lasers. Station positions used for RML are given in Appendix B and the compatible set of positions for the 3 NASA lasers was used. A timing bias of 550 μsec and a bias of 14 cm were applied to the RML data for Revs 3950 and 4340 whose residuals are shown in Figures 13 and 14. These biases were indicated by the data reductions discussed in Appendix B.

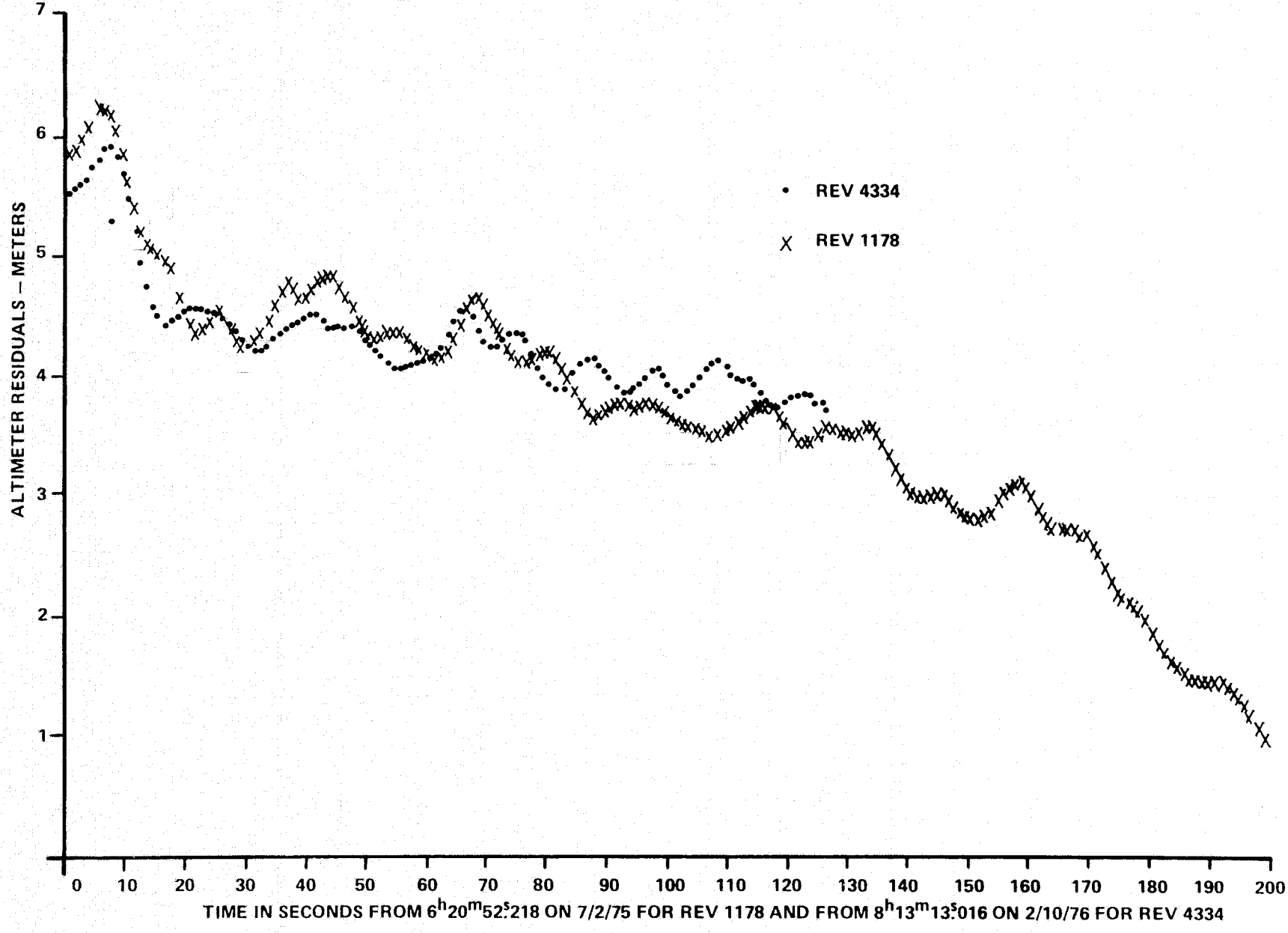

FIGURE 10. ALTIMETER RESIDUALS FOR OVERLAPPING TRACKS ON REVS 1178 AND 4334.
GROUNDTRACK SEPARATION IS 2.4 km

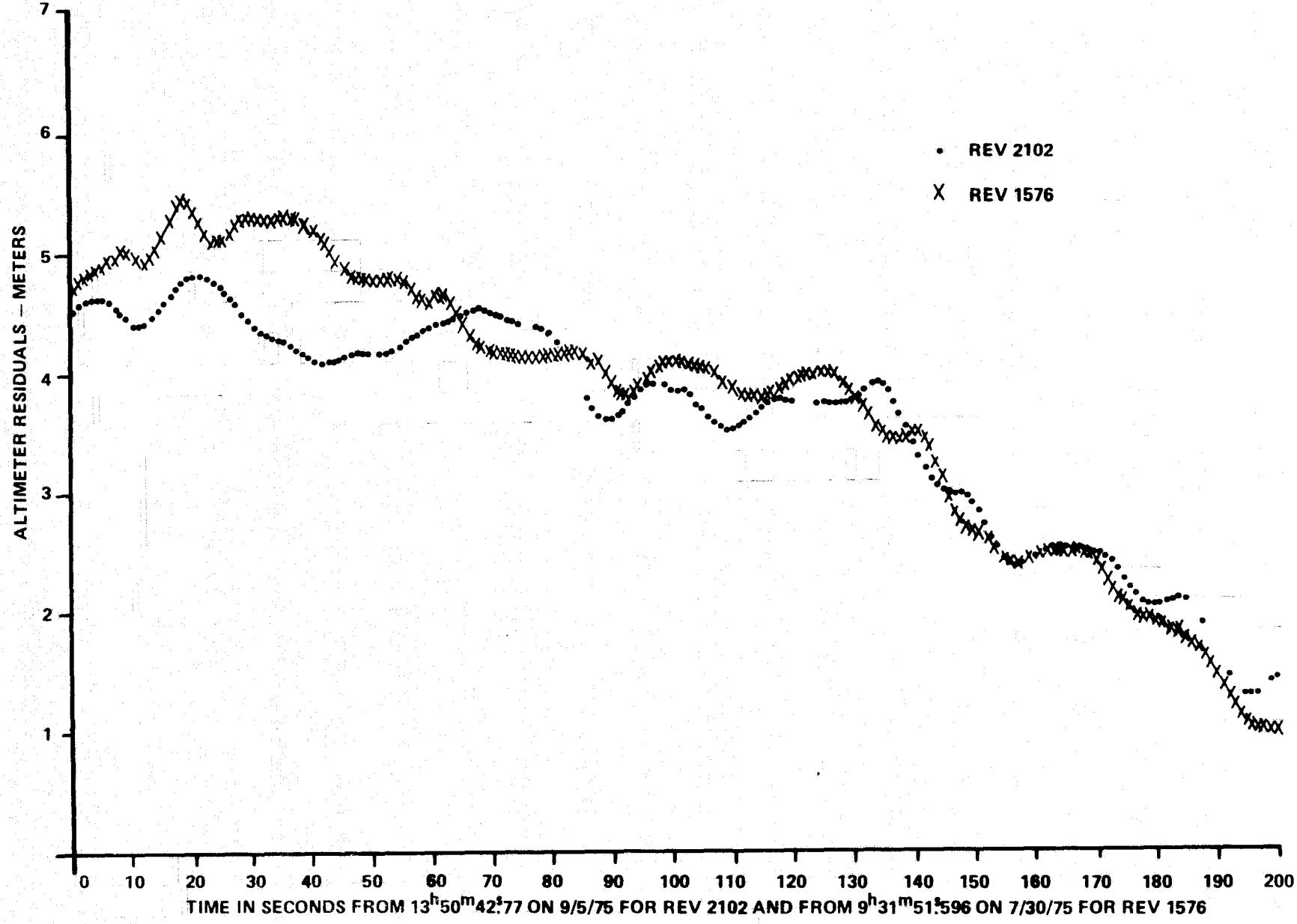

FIGURE 11. ALTIMETER RESIDUALS FOR OVERLAPPING TRACKS ON REVS 2102 AND 1576. GROUNDTRACK SEPARATION IS 2.1 KM.

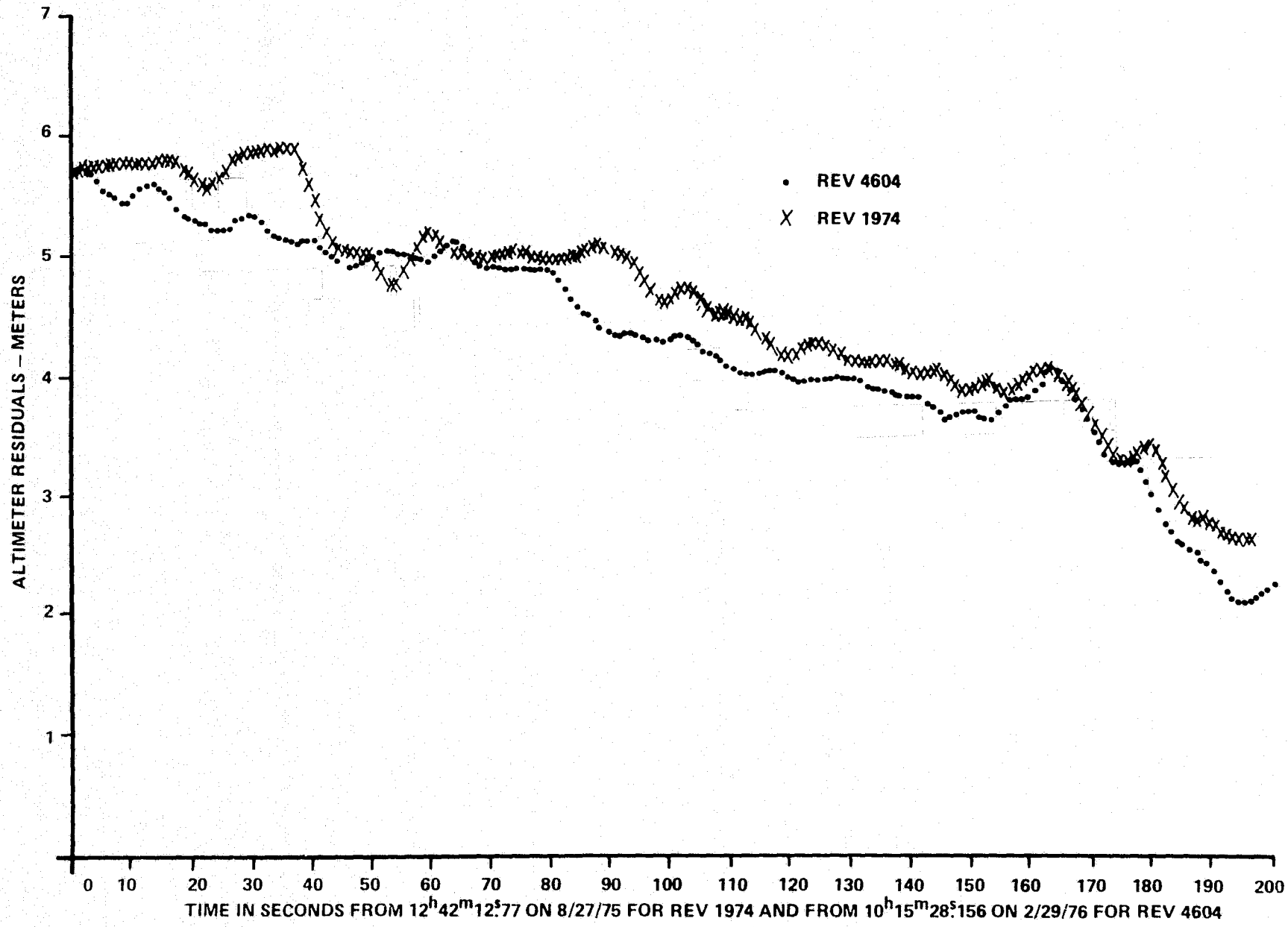

FIGURE 12. ALTIMETER RESIDUALS FOR OVERLAPPING TRACKS ON REVS 1974 AND 4604. GROUNDTRACK SEPARATION IS 5.3 km.

FIGURE 13. ALTIMETER RESIDUALS FOR OVERLAPPING TRACKS ON REVS 1710 AND 4340. GROUNDTRACK SEPARATION IS 2.9 KM.

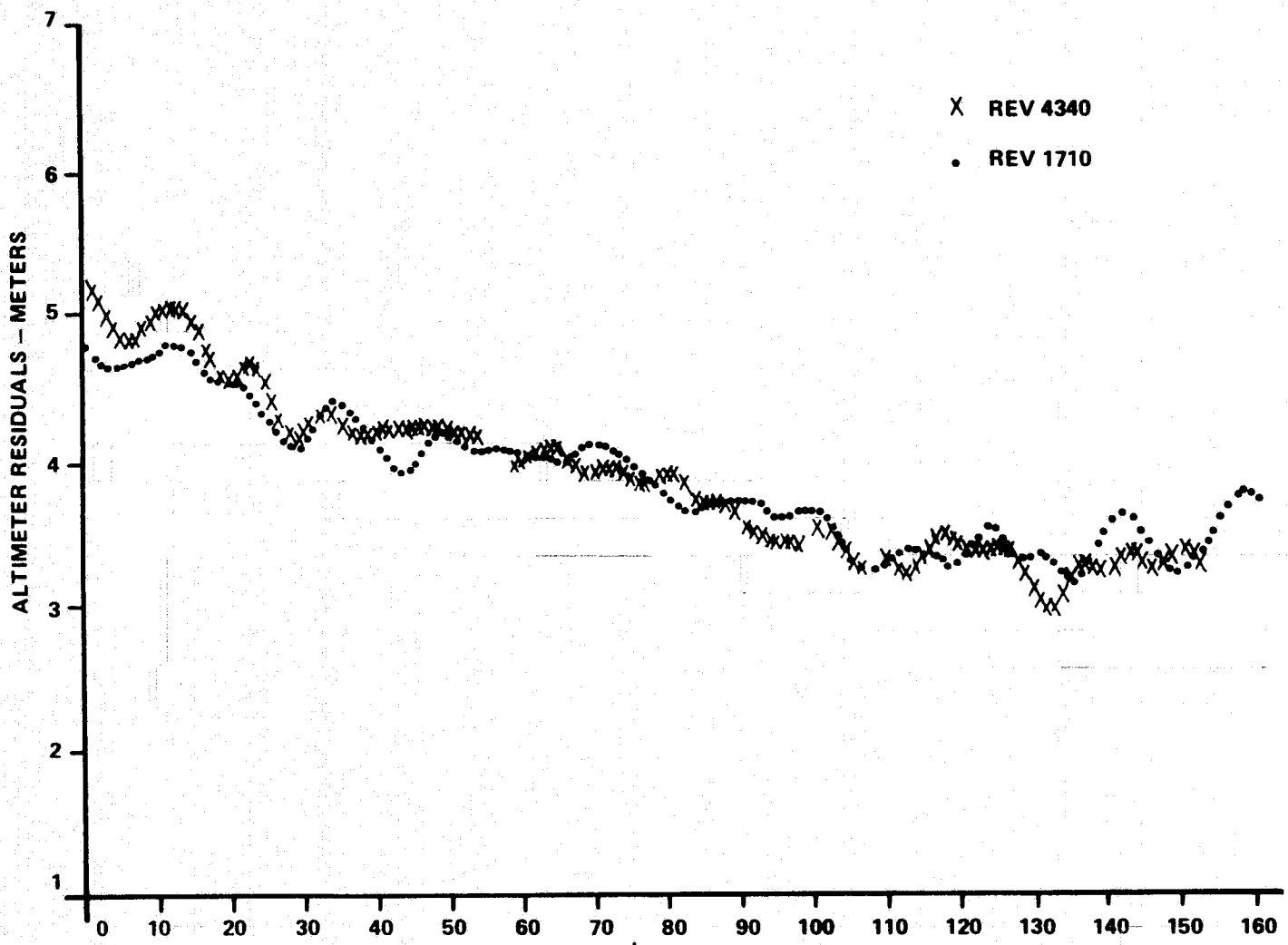

FIGURE 14. ALTIMETER RESIDUALS FOR OVERLAPPING TRACKS ON REVS 3950 AND 4476.
GROUNDTRACK SEPARATION IS 4.1 KM.

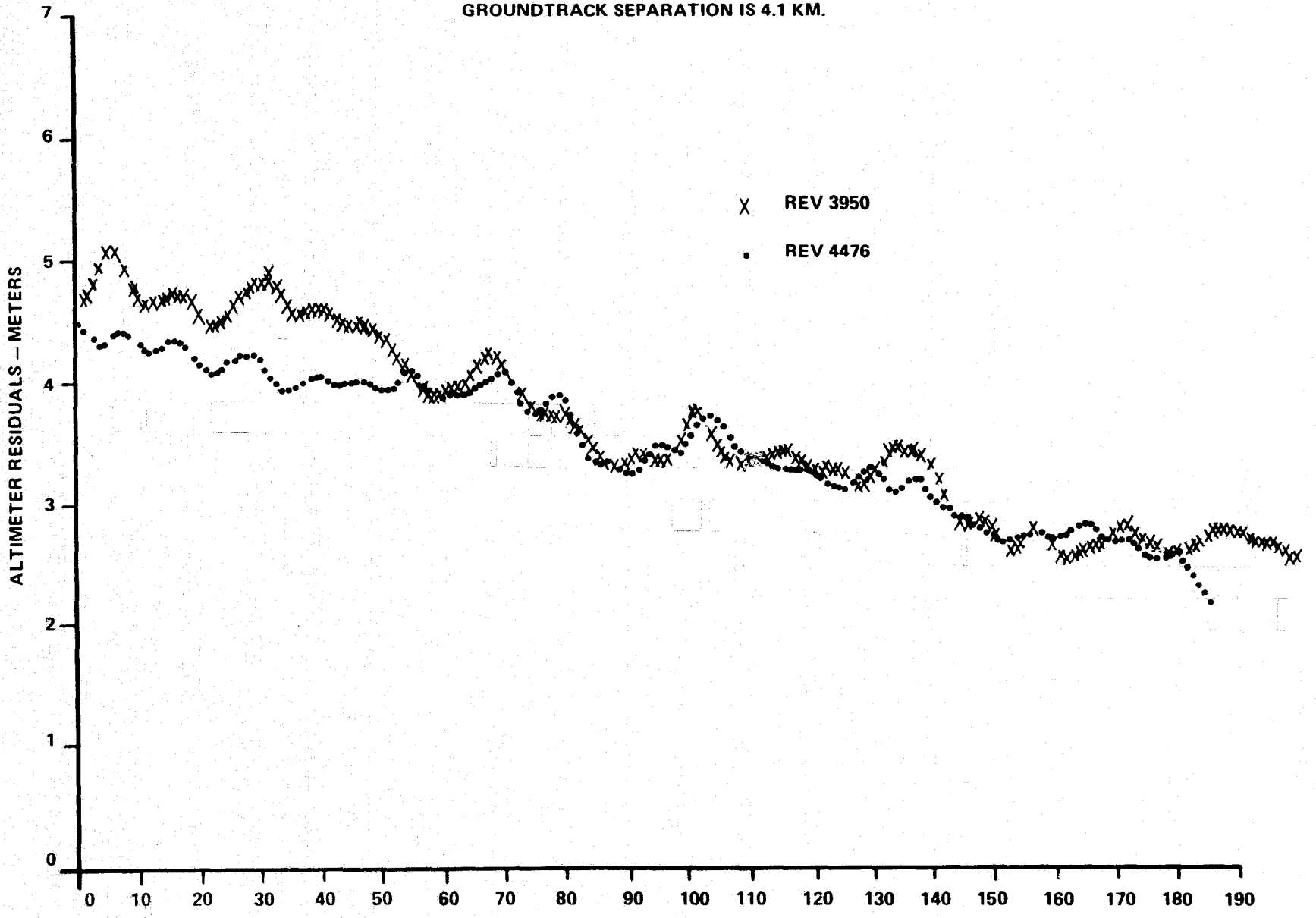

3.2.1 Bias Stability

If the scatter in the altimeter crossovers is to be interpreted as temporal sea surface height variations, the bias stability should be most reliably revealed from the overlapping tracks. In Figure 10, showing residuals for data taken in July 1975 and February 1976, there is no obvious offset between the two sets of residuals. There is a slight indication of an overall slope difference between the two passes, which could be indicative of a significant amount of orbit error. In Figure 11, showing residuals for data taken in July 1975 and September 1975, there is no evidence of a consistent offset between the two passes during the last 2 minutes. During the first minute, however, there are differences on the order of a meter for a distance in excess of 200 km, which could be due to a cold water eddy on Rev 1576 and not on Rev 2102. This explanation is certainly physically credible.

Figure 12 comes closest to showing a systematic difference between two different passes. Even here, however, the mean difference is only on the order of 20-30 cm, and there are several segments for which the two passes seem to be in much closer agreement. Overall, the differences are not considered to be too large to be explicable as some combination of orbit error, propagation error, and temporal sea surface height variations of a type which are known to exist at times in the calibration area.

Figure 13, showing residuals for Rev 1710 in August 1975 and Rev 4340 in February 1976 show almost perfect overall agreement. This set of passes comprise the only South-North overlaps included. It may be noted that the geographic area covered is mostly in the southern to central regions of the calibration area, where the other passes have also shown rather good agreement.

Figure 14 shows another set of passes for which the RML laser data was used to obtain one of the orbits. One of the passes, Rev 3950, is in January 1976 and the other, Rev 4476, is in February 1976. After the first minute, which again shows symptoms of an eddy on one of the passes, the two passes show perhaps the best agreement of any of the overlaps, with no indication whatsoever of a systematic offset between the two.

We thus conclude that the data shows no evidence of a significant bias variation between the times of Rev 1178 and Rev 4624. Assessment of the bias stability before Rev 1178 and after Rev 4624 would have to be done via the bias estimation method using the geoid model (see Section 3.1.1). However, Section 3.1.1 considered passes prior to Rev 1178, with no apparent bias variation between Revs 203 and 2244.

It may have been noticed that Figures 10-14 all show "high frequency" undulations with periods of about 10 seconds or 60-70 km. The question then arises as to whether or not these undulations correspond to physical undulations in the real sea surface. The answer to this question is that the large amplitude undulations are real, but that undulations of ~15 cm amplitude can exist due to measurement noise. This is demonstrated in Figure 15, which shows the effects of random noise of 72 cm amplitude (the average altimeter noise level, to be computed in Section 3.4) when passed through the filter used for the residuals shown in Figures 10-15. The amplitude and frequency of the undulations in Figure 15 is very similar to the high frequency oscillations in Figures 10-14, thus suggesting that the latter are due to measurement noise effects.

3.2.2 Timing Validation

Barring temporal sea surface height variations, verification that the correct time tags have been applied to the altimeter data can be performed through crossover analysis, since altitude

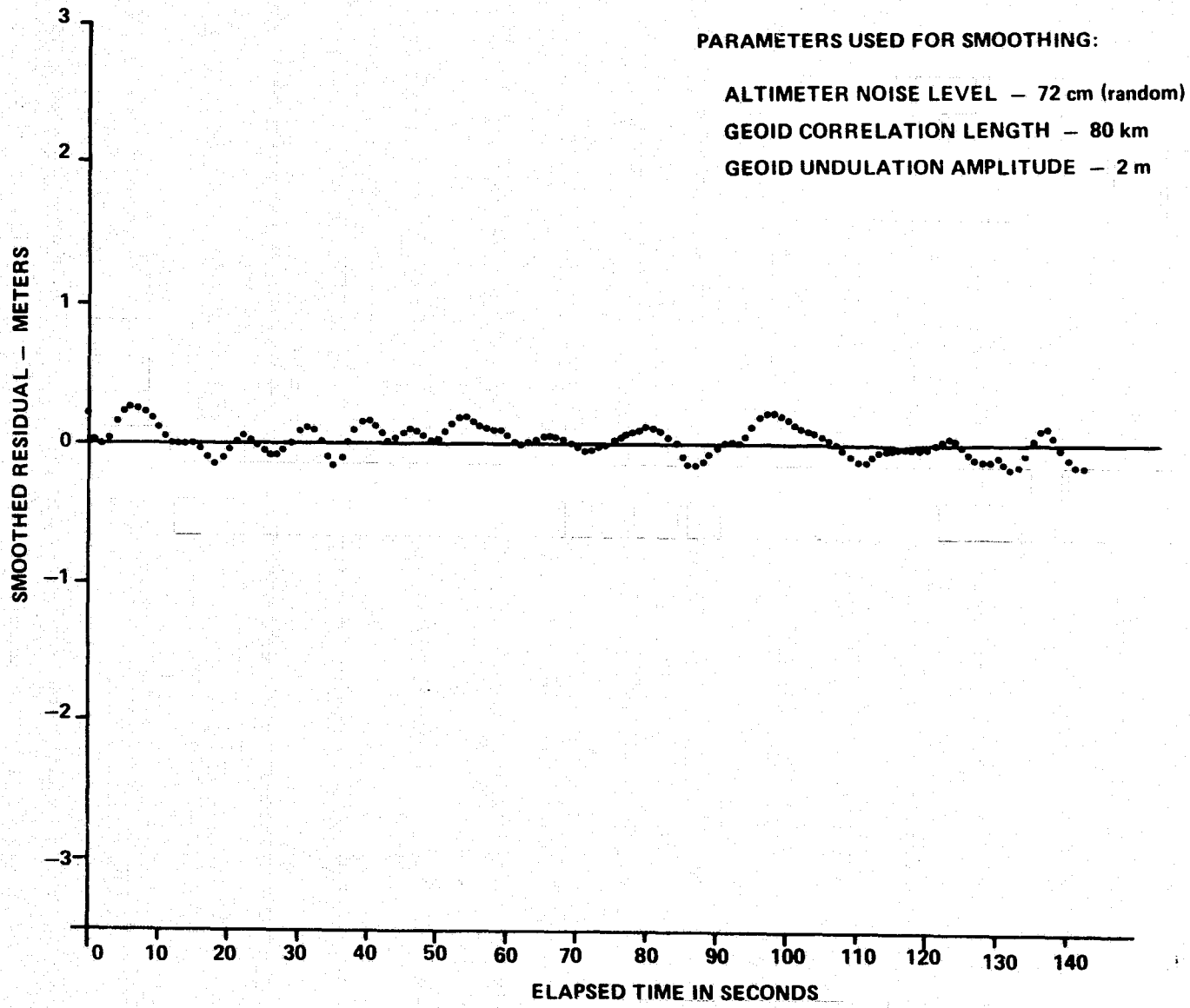

FIGURE 15. SMOOTHED ALTIMETER RESIDUALS DUE TO MEASUREMENT NOISE

rates for North-South and South-North passes are opposite in sign. The effects on altimeter residuals are not very large, however, since the altitude rates for the calibration area passes have magnitudes only in the range 10-30 m/sec. Nevertheless, a time tag error should exhibit itself in the form of a systematic bias in the crossover differences such as are shown in Figure 9. Indeed, we have already noted above that the mean crossover difference is -30 cm, suggesting that the North-South residuals are systematically too small, which could be due to the time tags being too small.

The overlapping passes shown in Figures 10-14 have shown, however, that temporal variations of a meter or greater can occur between passes, particularly in the northern portion of the calibration area, and the average crossover difference could be significantly affected by such variations. To minimize temporal effects on the crossovers, only the set of 4 crossovers consisting of passes 6-8 revs apart were examined. These crossovers are summarized in Table 4, with estimated corrections included for propagation effects. The two southernmost crossovers show residual differences after propagation corrections of 5 cm or less, which is more than consistent with measurement noise effects alone.

The other two crossovers must be explicable as indications of an actual timing error, an altimeter bias variation, orbit error, or a temporal variation in sea surface height between passes. Analysis of the 4604-4610 crossover using different sets of station positions (the largest contributor to orbit error) suggests that station position errors cannot be a large contributor to the observed 49 cm difference. Since no overlap showed real evidence of a bias variation, and the first two crossovers show no evidence of time tag errors, the most plausible explanation for the two discrepancies in Table 4 must be the passage of eddies into (or out of) the area between passes.

We thus conclude that the crossover differences shown in Table 4 are consistent with the altimeter data having been properly time tagged.

Crossover Revolution	Uncorrected Residual Difference	Propagation Correction		Net Residual Difference
		Tropospheric	Ionospheric	
1718-1710	-14 cm	+3 cm	+7 cm	-4 cm
2102-2094	0	-5 cm	0	-5 cm
4476-4482	-68 cm	~0	+7 cm	-61 cm
4604-4610	-54 cm	0	+5 cm	-49 cm

Table 4. Crossover Differences for Passes Half Day Apart, Including Approximate Corrections for Propagation Effects

3.2.3 Bias Variation With Telemetry Mode

In all the above discussion of intensive mode bias estimation, validation, and stability, essentially no mention has been made of telemetry mode. In fact, some of the data was taken in Telemetry Mode 1 and some in Telemetry Mode 2. Both of these modes transmit cumulative altitudes, which consist of on-board averaging of ten altitude measurements. This is the data that was used in all the above analysis.

In Telemetry Mode 3, however, "instantaneous" or individual altitude measurements are telemetered to the tracking stations. Keeney and Hofmeister of General Electric [17] have calculated, based on analysis of differences between spacecraft manipulation of instantaneous and cumulative altitude data, that the TM Mode 3 data should have a bias which is algebraically 47 cm smaller than the cumulative altitude data. Accordingly, an attempt was made to assess that the data is consistent with this bias difference.

No TM Mode 3 data exists through the calibration area with 3 laser tracking. A limited number of passes do exist, however, in which there was a transition within the pass from one telemetry mode to another. Two such transitions have been examined, and the altitude residuals before and after the TM mode change are shown in Figures 16 and 17. For these figures, the TM Mode 3 altitudes have been increased by 47 cm and have been averaged over groups of ten in ground data processing in order to produce equivalent cumulative altitudes.

In processing the Rev 246 data, the Marsh-Chang 5' x 5' geoid model was used, and the overall residual pattern shown in Figure 16 has no apparent trend. Rev 248 data did not pass through the GEOS-3 calibration area, and no geoid model was applied. The resulting residual pattern shows an overall linear trend, which would be expected on the basis of geoid

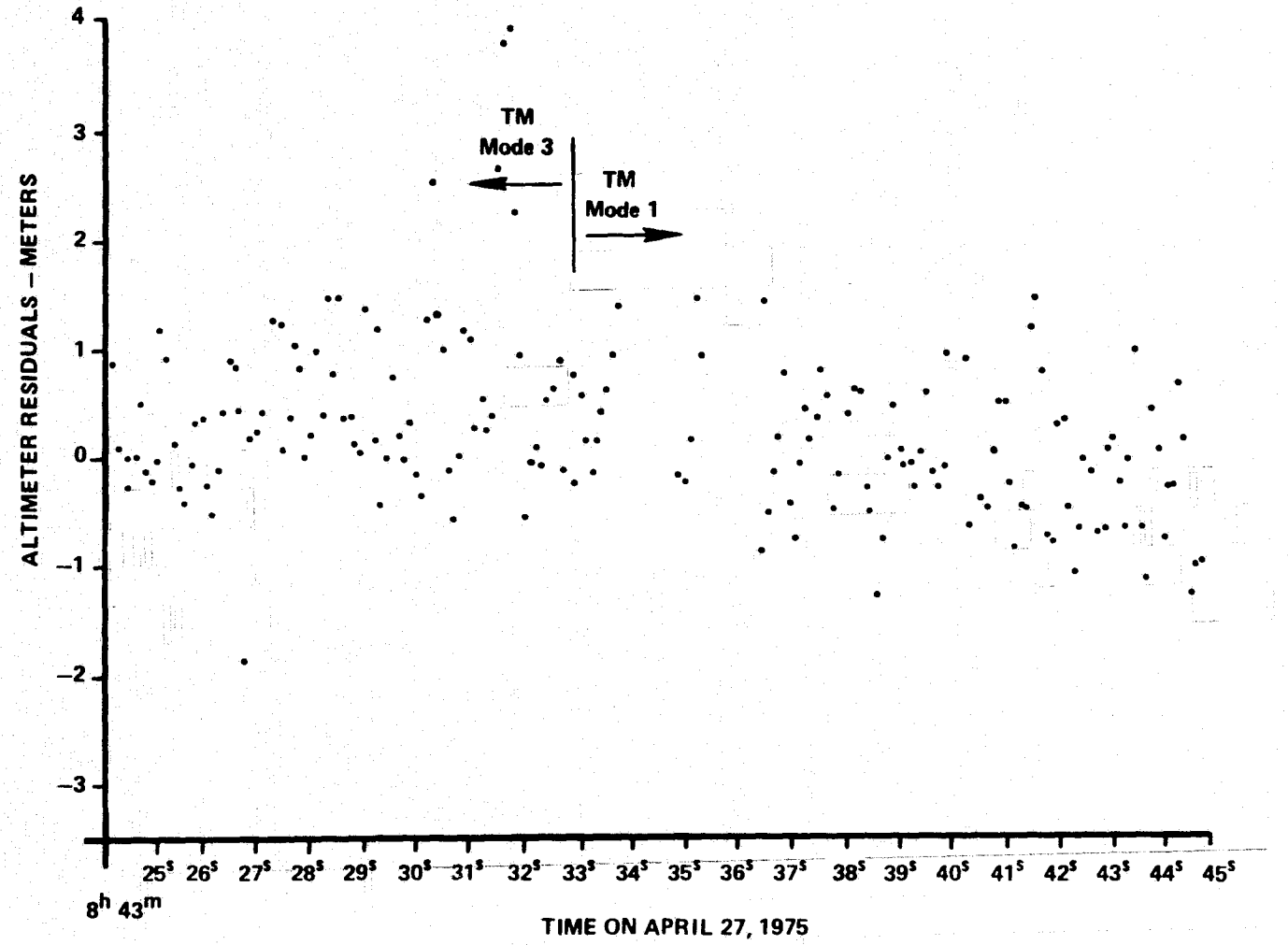

FIGURE 16. ALTIMETER RESIDUALS ON GEOS–3 REVOLUTION 246 ACROSS CHANGE IN TELEMETRY MODES

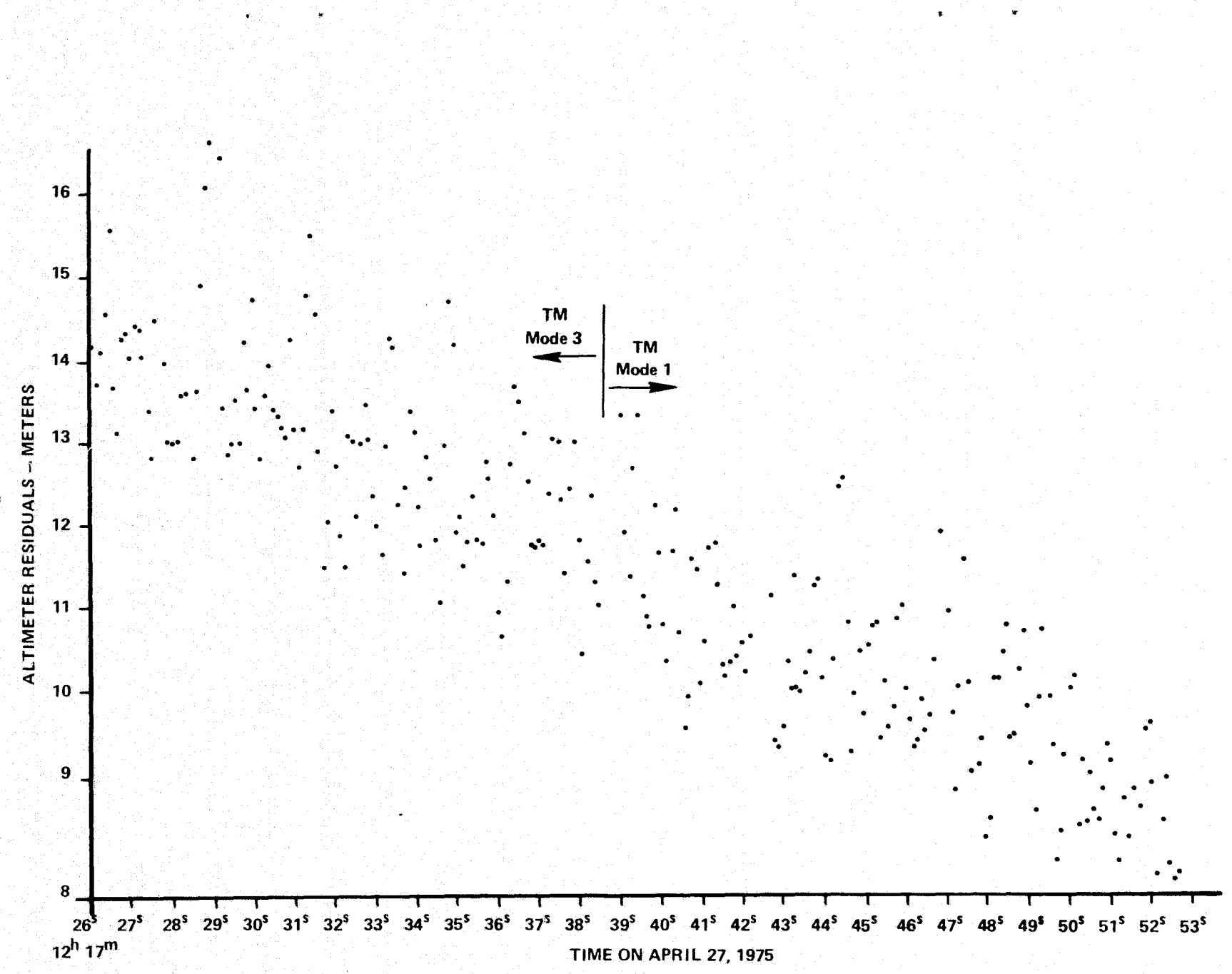

FIGURE 17. ALTIMETER RESIDUALS ON GEOS–3 REVOLUTION 248 ACROSS CHANGE IN TELEMETRY MODES

model and orbit error. There is no discernable change in the residual level at the time of the telemetry mode change for either pass, although the noise levels are sufficiently high that the visual test of consistency cannot be considered conclusive.

It should be noted that the time tagging of the TM Mode 1 and TM Mode 3 data was performed according to the procedures described in the GEOS-C Preprocessing Report [18], corrected as indicated in Appendix A of this report. Although it is again a rather weak confirmation, the consistency across mode changes in Figures 16 and 17 does indicate that the time tagging procedure is valid to within approximately 20 msec.

We conclude that the TM Mode 3 data appears consistent with the altitude bias (relative to TM Mode 1) calculated by G.E. and the time tagging procedure given in the GEOS-3 Preprocessing Report.

3.3 ANOMALOUS DATA PERIODS

Analysis of the GEOS-3 altimeter data has shown that there are times when the measurement is anomalously long by a magnitude on the order of 4-6 m for a time duration of several tenths of a second. In the process of smoothing residuals, all such periods that have been identified have been deleted and thus do not have any influence on the bias estimations or crossover analysis. However, if they are not deleted, spurious short wavelength undulations (of a meter or so in amplitude) will be introduced in the smoothed data.

Although the cause of these anomalies has not been definitively identified, certain of their characteristics are quite well known. Figure 18 shows the residuals for an anomalous data period on Rev 4553. On a different scale, these anomalous residuals have already been shown without

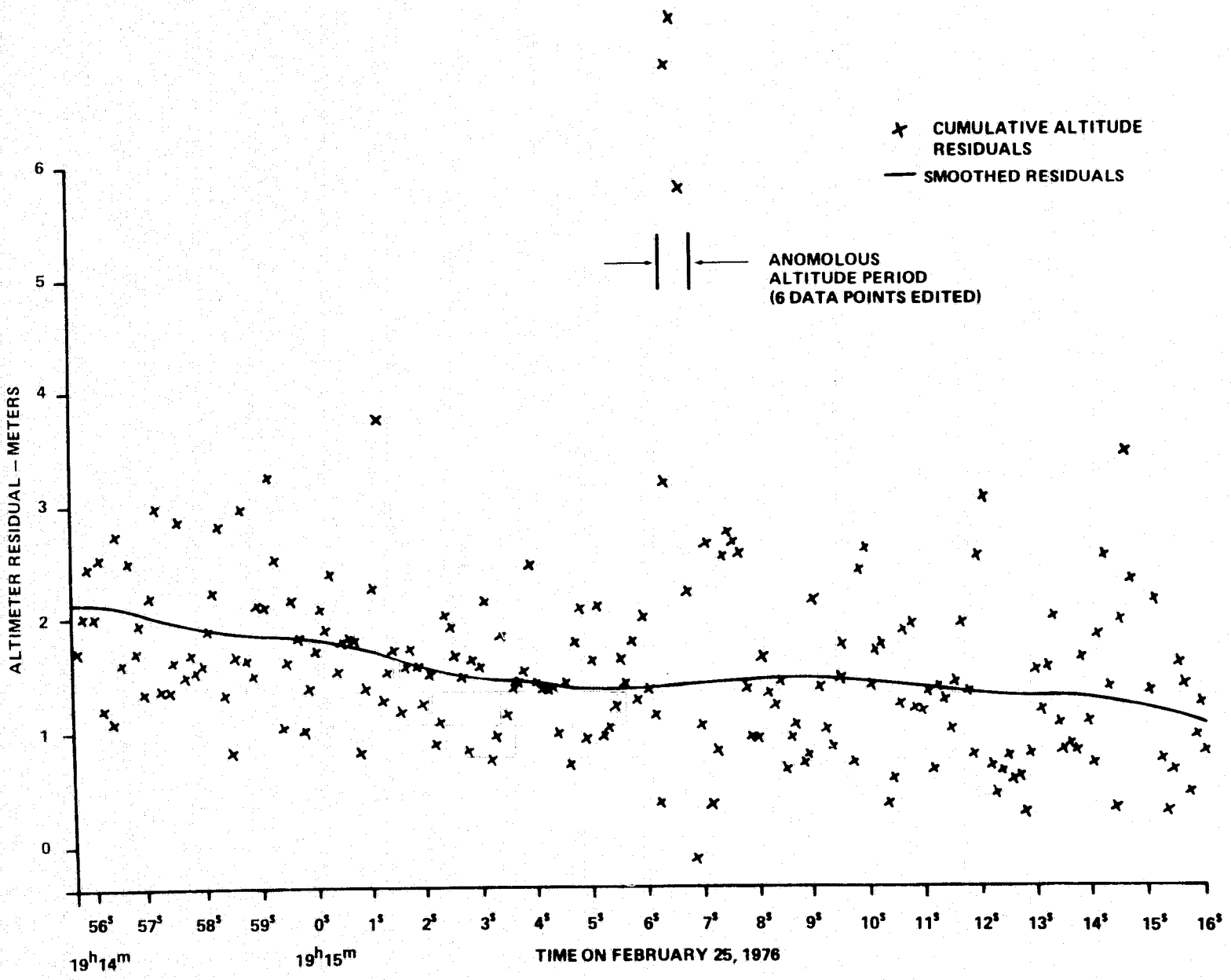

FIGURE 18. ALTIMETER RESIDUALS ACROSS ANOMALOUS DATA PERIOD. ANOMALOUS POINTS NOT USED IN COMPUTING SMOOTHED RESIDUALS

comment on the beginning of the plot in Figure 7. The anomalous period lasts for about 0.4 seconds as noted on Figure 18. Three cumulative altitudes during this period are rather clearly outliers from the rest of the residuals, and editing could be accomplished on this basis alone.

Further evidence that the points should be considered invalid is obtained from the waveforms during this period. Figure 19 depicts in 3 dimensional form the return waveforms during the period around the anomaly. The points plotted in Figure 19 are obtained from averaging 5 instantaneous waveforms.* As may be seen in the Figure, the anomalous period is characterized by excessive (i.e., above noise level) energy return in the early gates, starting as early as Gate 2. In some of these waveforms, there is also a valley in the vicinity of the Ramp Gate (No. 10).

Both of these features are perhaps more clearly evident in Figure 20, which shows some waveforms in the immediate vicinity of the anomaly. Each of the waveforms shown is a 10 sample (~.1 sec) average. The first waveform shown is reasonably normal. In the second and third waveforms, the leading edge of the return pulse can be seen to move closer to Gate 1, until Gate 2 has a visibly abnormal return in the fourth waveform. In the following waveforms, the return pulse becomes later and later until it appears to be near the normal time in the seventh waveform. The valley mentioned above is most evident in the fourth and fifth waveforms, with Gate No. 10 located near the minimum. In the sixth waveform, however, Gate 10 is on a peak, which should indicate to the tracking algorithm that the gates should be moved forward in time. In the last two waveforms, this movement has taken place.

---

*Rev 4553 is a TM Mode 2 pass and waveform data is thus available at the ~100 samples/second rate.

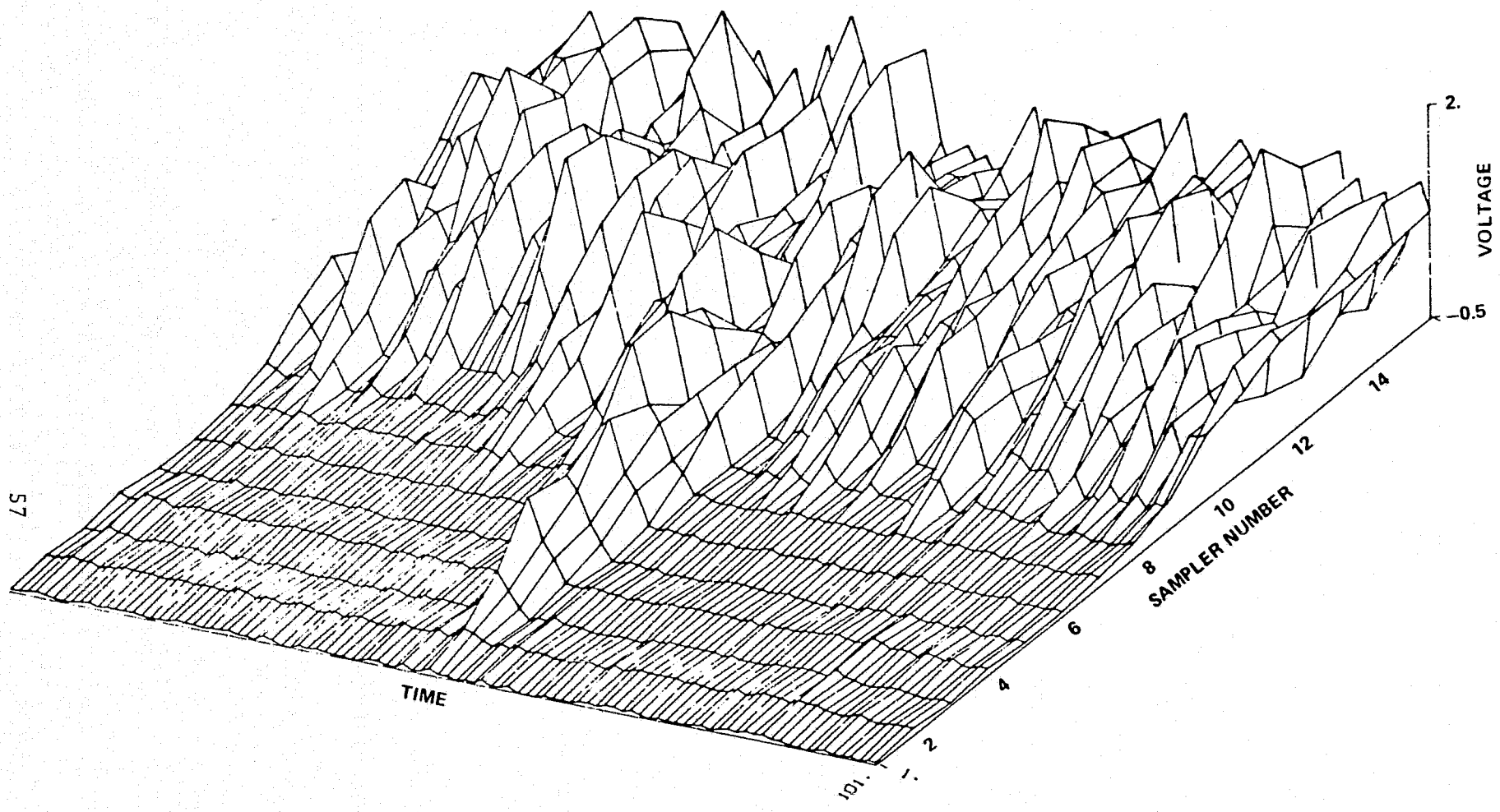

FIGURE 19. THREE DIMENSIONAL WAVEFORM IN THE VICINITY OF AN INTENSIVE MODE ALTITUDE ANOMALY. GRAPHED POINTS ARE 5 SAMPLE AVERAGES.

FIGURE 20. TEN SAMPLE (.1024 SECOND) AVERAGES OF WAVEFORMS IN THE VICINITY OF AN ALTITUDE ANOMALY

No attempt has been made to compile any statistics as to the frequency of the ~6 m anomalies, but almost all of the passes analyzed contained at least one. A ballpark estimate of frequency would be ~1/minute. Some question has also arisen as to the existence of ~3 m anomalies. However, no study has been made to determine whether data points deviating by ~3 m from the local mean should be considered anomalies, or may be satisfactorily treated as measurement noise. No such data periods were edited in any of the smoothing operations. However, depending upon the origin of the 6 m anomalies, 3 m anomalies could very well also exist.

3.4 DATA NOISE LEVELS

In the process of smoothing the altimeter data to perform the crossover analysis, the root sum of squares (rss) of the raw measurements about the smoothed data were also calculated. These numbers should be very nearly the measurement noise levels, and are summarized in Table 5 on a pass by pass basis. All the "6m anomalies" have been deleted before the computation of the rss.

Typical data used in the computation is that shown in Figure 18, with the rss computed about the smoothed residuals and the anomalous data segment deleted. Overall, the computed noise level is 72 cm, with a range from 57 cm on Rev 4604 to 82 cm on Revs 4334 and 4462. It is of some interest that the lowest rss was obtained for a pass for which there is some suspicion of having slightly anomalously short measurements. Indeed, such a correlation should exist if the tracking for the pass were near specular. However, examination of the waveforms for this pass gives little support to the hypothesis that the return pulses for 4604 are significantly different than for the other passes.

Revolution	No. of Points	RSS (cm)
1178	2200	76
1576	2091	77
1710	1632	79
1718	2300	74
1974	2260	64
1988	2395	67
2094	1720	74
2102	1917	81
2151	2020	71
4334	1395	82
4391	576	74
4462	346	82
4476	1882	68
4482	1952	77
4553	1452	66
4604	2336	57
4610	1760	68
4624	1441	67
Total	31675	72

Table 5. Root Sum of Squares of Raw Cumulative Altitudes About Smoothed Altitudes

3.5 INTENSIVE MODE BIAS ACCURACY ANALYSIS

As indicated in Section 3.1.2, the most accurate calibration for the GEOS-3 altimeter intensive mode is considered to be the overhead calibration for Rev 4553. The error sources which are expected to have an effect on this calibration are listed in Table 6, along with their estimated magnitude and the corresponding contribution to the uncertainty in the calibration accuracy.

It will be noted from Table 6 that

1. The overwhelmingly dominant error source is measurement noise.

2. There is no geoid model term listed.

As has been pointed out in Section 3.1.2, the calibration method inherently avoids the need for a geoid model, but at the expense of a larger error contribution from measurement noise since, in essence, the data is required to determine the local ocean geoid and extrapolate to the tracking site. If an error free geoid model were available, the altimeter noise contribution to calibration accuracy could be reduced to no more than the few centimeter level, although there would then be a non-negligible contribution from station position errors.

Many of the 5 cm error sources included in Table 6 are upper limits and may have considerably smaller magnitudes. E.g., there is no evidence for a laser bias, but the normal specifications for the laser accuracy are that the bias does not exceed the noise level which is on the order of 5 cm. Any Bermuda bias would propagate directly into the estimated altimeter bias.

Error Source	Magnitude of Assumed Error	Effect on Estimated Altimeter Bias
Altimeter Noise	72 cm	18 cm
Tropospheric Propagation	2%	5 cm
Ionospheric Propagation	50%	5 cm
Ground Tracker Noise	5 cm for each laser station	2 cm
Ground Tracker Bias	5 cm at Bermuda	5 cm
Tides	5 cm	5 cm
Station Position Error	20 cm baselines 1 m heights	<3 cm
Sea State/ Off-Nadir Effects	Wave height <1 m Off-nadir angle <0.5°	<5 cm
Total		21 cm

Table 6. Error Components for Rev 4553 Overhead Calibration

Finally, we may compare the estimated bias from Rev 4553 with the bias currently estimated by G.E. [1,17] on the basis of calculated spacecraft delays within the altimeter hardware and in data transfer. Referencing the G.E. value to the spacecraft center-of-mass to be consistent with our estimated bias, we have for the intensive mode cumulative altitudes:

G.E. Bias Estimate*	-6.08 m $\pm$ .5 m
Rev 4553 Bias Estimate	-5.30 m $\pm$ .2 m

These values are very close to agreement within 1σ, and we would thus consider them to be consistent.

*This value differs from the number given in Section 1 by 47 cm, the G.E. computed difference between biases for TM Mode 3 and TM Modes 1 and 2. Since the existence of a bias difference was not determined until subsequent to the preparation of Ref. 2, the earlier number was referenced in Section 1. Data taken on Rev 4553 was in TM Mode 2.

SECTION 4.0
GLOBAL MODE CALIBRATION

The procedure which has been adopted for the estimation of the GEOS-3 altimeter global mode bias has been heavily influenced by

1. The existence of intensive mode passes with relatively well determined orbits (from 3 laser tracking).

2. The approximately 1 m discrepancy between the intensive mode biases estimated from the Bermuda overhead pass (Section 3.1.2) and the set of passes based upon the geoid model (Section 3.1.1).

Thus, if satisfactorily good orbits can be obtained for the global mode passes, the crossovers with the intensive mode passes discussed in Section 3.2 can be used for global mode bias estimation. Using this procedure, systematic geoid model errors will not influence the results.

Section 4.1 presents the comparisons of the global mode passes with the previously presented intensive mode passes. Based on these comparisons, an estimate is made of the global mode bias. Sections 4.2 - 4.4 then analyze the global mode results to assess the bias and overall data accuracy.

4.1 BIAS DETERMINATION

Two types of comparisons of global mode and intensive mode passes are possible. In addition to the crossovers, the groundtracks for some of the global and intensive mode passes

lie within less than a footprint diameter, thus allowing a bias estimation on the basis of the shift necessary to make the global mode pass agree with the intensive mode pass. The opportunity is also presented for comparing the abilities of the two modes for measuring short wavelength sea surface features. Whenever overlaps are possible, they will be used in place of the crossovers, although both will be computed in order to establish the consistency of the two methods.

A total of 14 global mode passes have been utilized in the bias estimation process, 7 North-South passes and 7 South-North passes. This set of passes is complete in terms of passes through the calibration area with sufficient ground tracking for satisfactory orbit estimation. Geometrically, the tracking requirements were that there be tracking by at least two calibration area ground stations (C-Band radar and/or laser), and that the satellite groundtrack pass between two of the tracking stations. ORAN analysis shows that orbit errors for these 14 passes will be expected to vary approximately linearly through the calibration area, with the slope dependent upon the actual measurement biases and station position errors, as well as the geometry of the pass relative to the tracking stations. The existence of large trends in the crossover differences along a global mode pass should thus be indicative that orbit errors are indeed present and that the pass should be used with caution.

Figure 21 shows the crossover differences* between the North-South global mode passes and the South-North intensive mode passes. Figure 22 shows the corresponding crossovers for the South-North global mode passes and the North-South

*Crossover differences are the differences between residuals for the North-South passes and for the South-North passes. Residuals are observed altitudes minus computed altitudes, with corrections included for tides and tropospheric propagation effects.

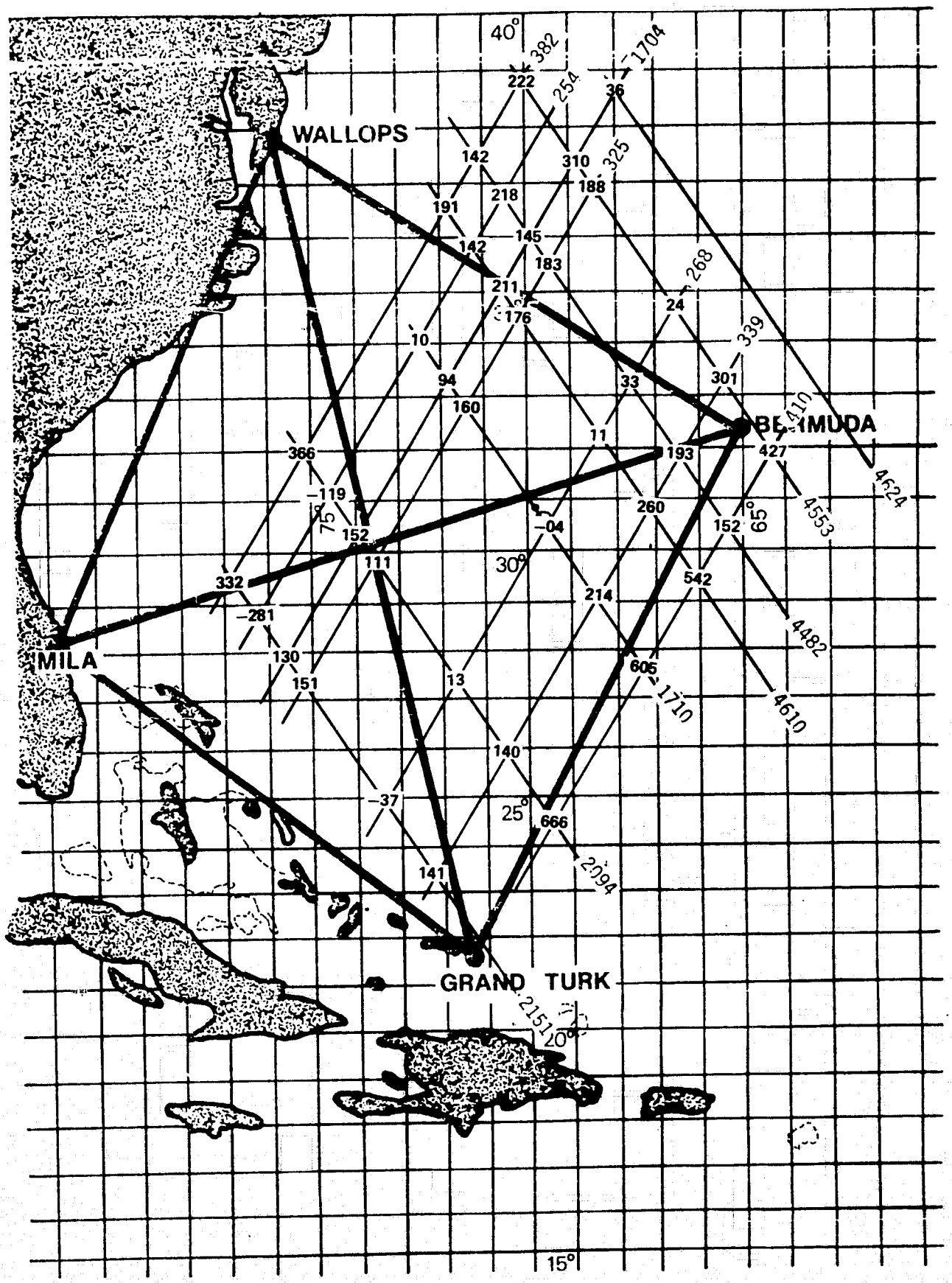

FIGURE 21. ALTIMETER CROSSOVERS, N–S GLOBAL MODE PASSES MINUS S–N INTENSIVE MODE PASSES. MEASUREMENT DIFFERENCES ARE IN CENTIMETERS.

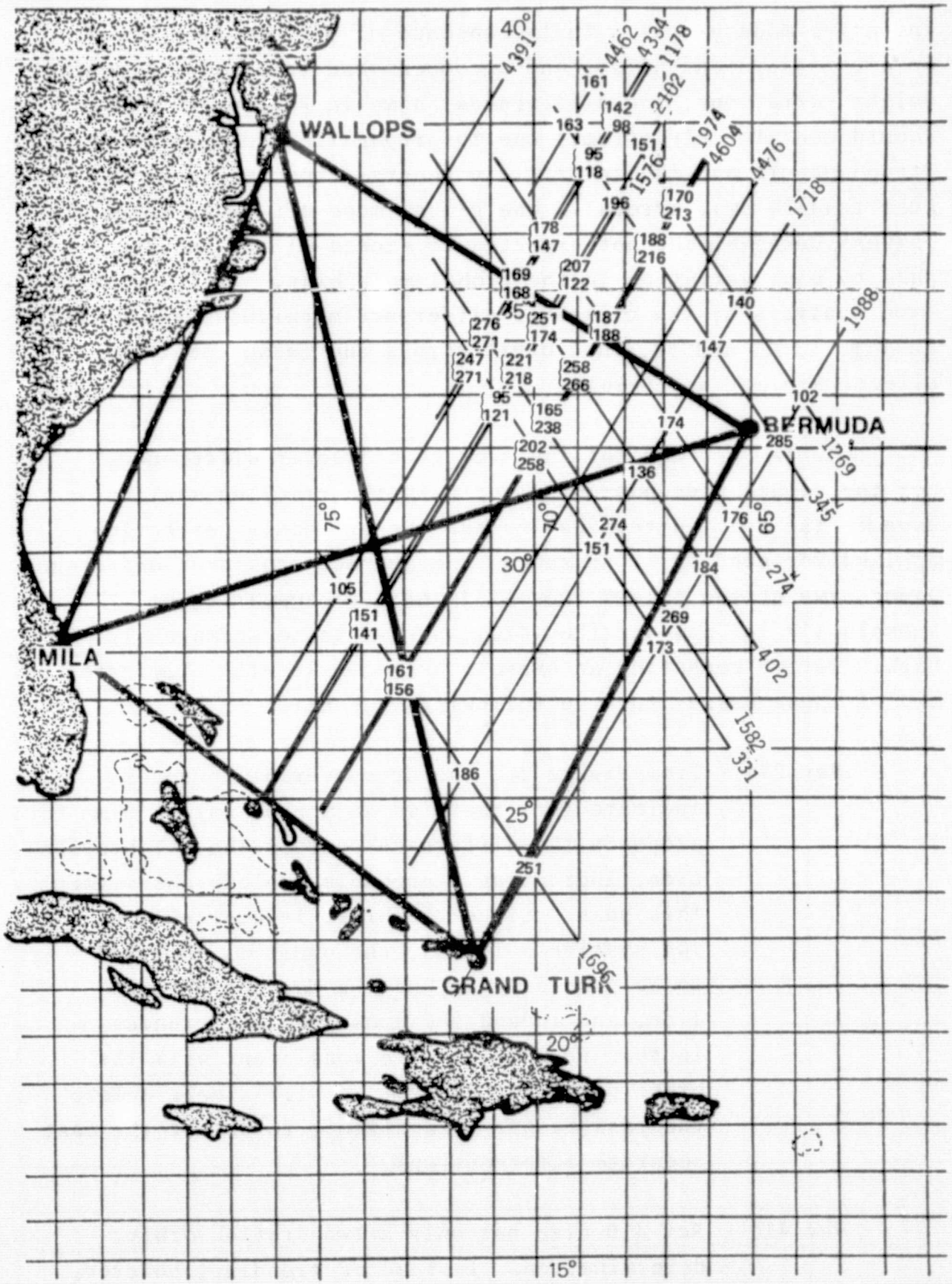

FIGURE 22. ALTIMETER CROSSOVERS, S–N GLOBAL MODE PASSES MINUS N–S INTENSIVE MODE PASSES. MEASUREMENT DIFFERENCES ARE IN CENTIMETERS.

intensive mode passes. In the absence of effects from orbit error, measurement noise, and uncompensated temporal sea surface height variations, the differences shown in Figures 18 and 19 should contain only effects due to propagation correction errors (tropospheric and ionospheric, in general expected to total less than 20 cm), errors in the global mode off-nadir model (amount unknown, but not expected to exceed ~1 m), and any pass to pass variation in the global mode bias. It is apparent, from analysis of the crossover difference magnitudes and patterns in Figures 21 and 22, that orbit errors and measurement noise effects are not negligible.

Table 7 summarizes the average crossover differences for the global mode passes, along with the tracking stations used in the orbit determination and the off-nadir correction applied for each pass. Based on the average crossover difference alone, two of the passes (Revs 254 and 268) appear to be anomalously low and one (Rev 410) appears to be anomalously high. Before computing an overall average, we will eliminate two of these passes for the following reasons:

Rev 254 - From Figure 21, the crossover differences indicate that there is an approximately 5 m slope in the differences across the calibration area, indicating a probable orbit problem for this pass. Since the orbit is basically a two station solution, the orbit is expected to be good only around the Wallops-Bermuda line, and indeed the crossover differences in this region are more consistent with the other passes. However, we will simply delete the pass rather than attempt to select the most accurate intersections.

Rev 410 - Rev 410 also has only a two station orbit determination. Instead of trending, however,

Rev No.	Direction	Tracking Stations Used For Orbit Determination	Computed Off-Nadir Angle/ Correction	Average Difference from Crossovers with Intensive Mode Passes
254	N-S	WAL/BDR/STA	0.77°/-1.55 m	-.06 m
268	N-S	WAL/BDR/GRT	0.92°/-2.30 m	.07 m
274	S-N	WAL/BDR/GRT	0.74°/-1.44 m	1.72 m
325	N-S	WAL/BDR	1.24°/-4.34 m	1.61 m
331	S-N	WAL/BDR/STA	0.74°/-1.45 m	1.90 m
339	N-S	WAL/BDR	0.92°/-2.32 m	2.08 m
345	S-N	WAL/BDR	0.73°/-1.38 m	1.76 m
382	N-S	WAL/BDR	1.18°/-3.95 m	2.50 m
402	S-N	WAL/BDR/STA	0.80°/-1.71 m	2.01 m
410	N-S	WAL/BDR	0.90°/-2.68 m	4.78 m
1269	S-N	WAL/BDL/GRT	0.80°/-1.72 m	1.47 m
1582	S-N	WAL/BDR/STA/GRT	0.73°/-1.39 m	2.41 m
1696	S-N	WAL/STA/GRT	0.88°/-2.10 m	1.63 m
1704	N-S	WAL/BDL/GRT	0.95°/-2.47 m	1.54 m

Tracking Station Legend:

WAL - Wallops Island C-Band radar (FPS-16 or FPQ-6)
BDR - Bermuda FPQ-6 C-Band radar
STA - Goddard stationary laser
BDL - Bermuda laser
GRT - Grand Turk laser

Table 7. Average Crossover Differences of Global Mode Passes with Intensive Mode Passes

the crossover differences show primarily excessive scatter. In large measure, this scatter is attributable to altitude anomalies in the data, near the time of Bermuda passage, whose effects were not completely eliminated from the smoothed data. These anomalies consist primarily of two ~10 m anomalies separated by about 30 seconds in time, but with a third anomaly of ~6 m amplitude within the 30 second span. These anaomlies are no doubt related to an ~10 db enhancement in AGC in this region, but no detailed analysis has been made to further pin down the reason for the observed altitude behavior. Since the residuals away from Bermuda are suspect because of the two station orbit estimation, it was decided to also eliminate Rev 410 from the bias estimation process.

Although Rev 268 may indeed have a couple of meters of orbit height error, its agreements with the intensive mode passes are very consistent, and there is no real basis for eliminating the pass.

As indicated above, several of the global mode passes have near overlapping groundtracks with one or more of the intensive mode passes. One such global mode pass is Rev 1704, whose groundtrack is only about 3.7 km from that of Rev 1178, an intensive mode pass. Figure 23 shows the smoothed residuals for these two passes after a shift of 1.75 m for Rev 1704 to obtain the best overall agreement between the two passes. Rev 1704 had 3 laser tracking, as did Rev 1178, and so their orbit errors should be very nearly the same. The 1.75 m figure is seen to be only 21 cm different from the crossover average.

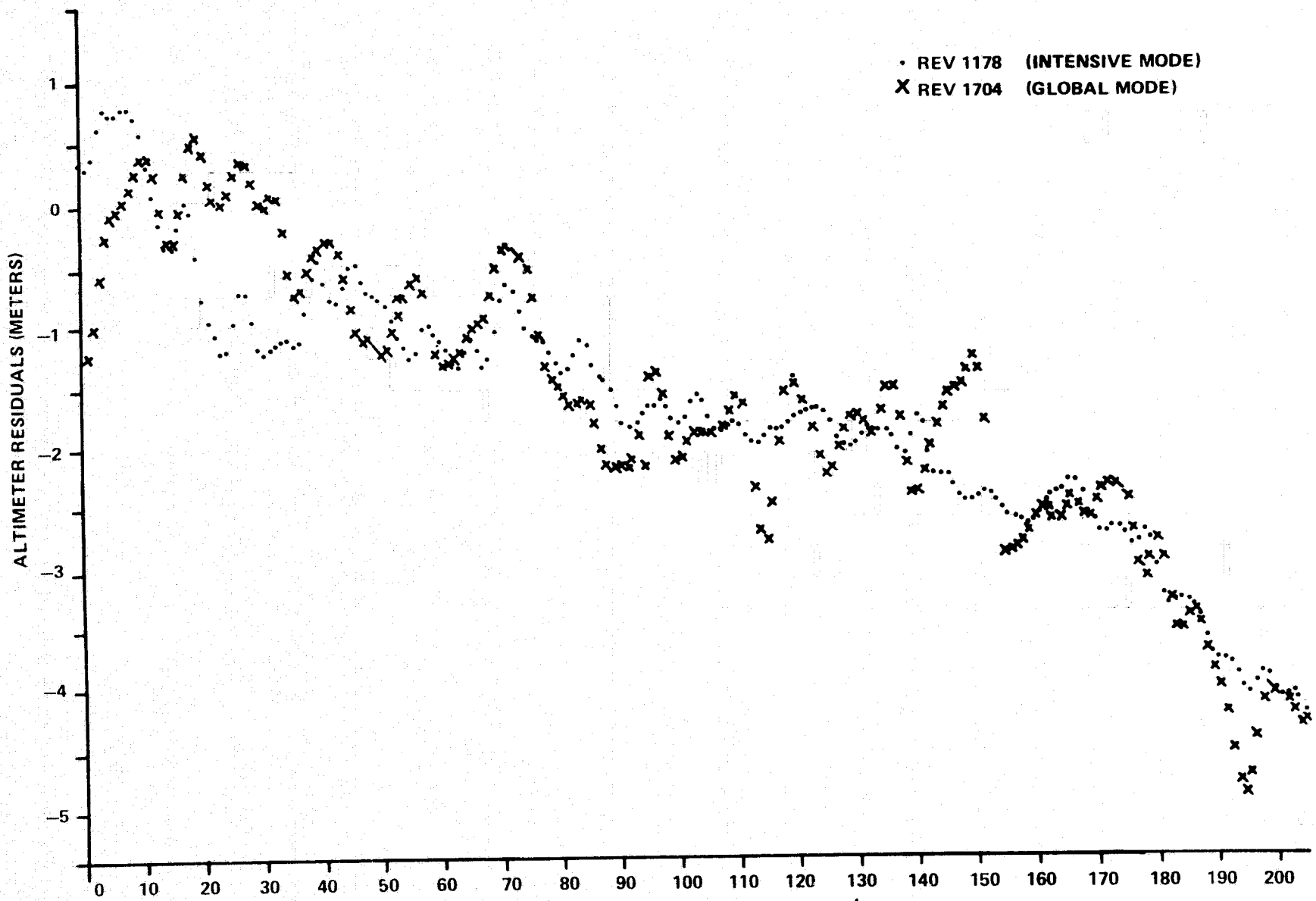

FIGURE 23. ALTIMETER RESIDUALS FOR OVERLAPPING TRACKS ON REVS 1178 AND 1704.
REV 1704 HAS BEEN SHIFTED DOWN 1.75 m.

Table 8 summarizes the differences of the remaining 12 global mode passes from the intensive mode crossovers or overlaps. In general, the overlaps are considered to be somewhat more accurate and are used for those 3 passes for which they are available. The result, giving equal weight to all the passes, shows the global mode bias to be 1.75 m larger (algebraically) than the intensive mode bias. This number turns out to be exactly the same as that given by the 1178-1704 overlap, which is gratifying even though it is only fortuitous.

Our best estimate of the global mode bias is then -5.30 m + 1.75 m = -3.55 m. This number should be used to correct the measurements to the spacecraft center-of-mass, assuming that an off-nadir correction is made separately.

4.2 BIAS STABILITY AND VALIDITY OF OFF-NADIR MODEL

For the twelve global mode bias differences listed in Table 8, the rms scatter about the mean is 62 cm. If Rev 268 is deleted, the rms is only 36 cm, although the mean increases to 1.90 cm. The latter rms could be expected on the basis of orbit error alone, so the 11 passes do not show any real evidence of bias variation with time. Rev 268, however, does appear to be almost 2 m different from the other 11 passes. This pass, along with Rev 410, are the only ones that show evidence of deviating from the 11 passes that are grouped together within a standard deviation of 36 cm.

In the process of assessing the pass to pass bias stability, it is necessary to take into account that a correction has been applied for the effects of the GEOS-3 antenna pointing in a direction other than nadir. The off-nadir angle itself has been calculated from measured characteristics of the return

Rev No.	Bias Difference From Intensive Mode	Source of Difference
268	.07 m	Crossovers with 6 intensive mode passes
274	1.72 m	Crossovers with 8 intensive mode passes
325	1.61 m	Crossovers with 6 intensive mode passes
331	1.90 m	Crossovers with 8 intensive mode passes
339	2.08 m	Crossovers with 6 intensive mode passes
345	2.40 m	Overlap with Rev 4553
382	2.50 m	Crossovers with 5 intensive mode passes
402	1.50 m	Overlap with Rev 4610
1269	1.47 m	Crossovers with 8 intensive mode passes
1582	2.41 m	Crossovers with 8 intensive mode passes
1696	1.63 m	Crossovers with 7 intensive mode passes
1704	1.75 m	Overlap with Rev 1178
Av. =	1.75 m	

Table 8. Summary of Components of Global Mode Bias Estimate

pulse (ratio of average "attitude-specular" gate voltage to average "plateau" gate voltage) during the pass. In particular, the algorithm [12] for using this voltage ratio to estimate the off-nadir angle does not compute an off-nadir angle less than about 0.70°, and has been suspected of being biased.* To investigate possible deficiencies in the off-nadir model, Figure 24 shows the 12 global mode biases from Table 8 as a function of off-nadir angle. The only obvious systematic behavior seen in this figure is that the South-North passes all have (computed) off-nadir angles which are less than any of the North-South passes. Most importantly, after eliminating the Rev 268 point, there does not appear to be any systematic relationship between the bias and off-nadir angle. This could be interpreted as meaning that if the computation of an off-nadir correction is in error, the error is a constant rather than being a function of off-nadir angle.

It may be further noted from Figure 24 that the Rev 268 point is at an intermediate value of off-nadir angle, which strongly suggests that the slightly anomalous bias for this pass is not due to off-nadir effects. Since an off-nadir correction of -2.3 m has been added to the Rev 268 bias as a correction for off-nadir pointing, it cannot be completely ruled out that the off-nadir algorithm has computed an excessively large off-nadir angle. Other explanations, however, appear to have a higher probability.

In summary, then, all but 3 of the set of 14 global mode passes give results which appear randomly distributed about the mean. Of the 3 exceptions, one (Rev 254) has been identified as having characteristics strongly indicative of

*The suspicion stems in part from the fact that the corresponding algorithm for intensive mode data frequently estimates an off-nadir angle less than 0.5°. The accuracy of the on-board attitude sensors [9] is insufficient to resolve the question, and no other information is available.

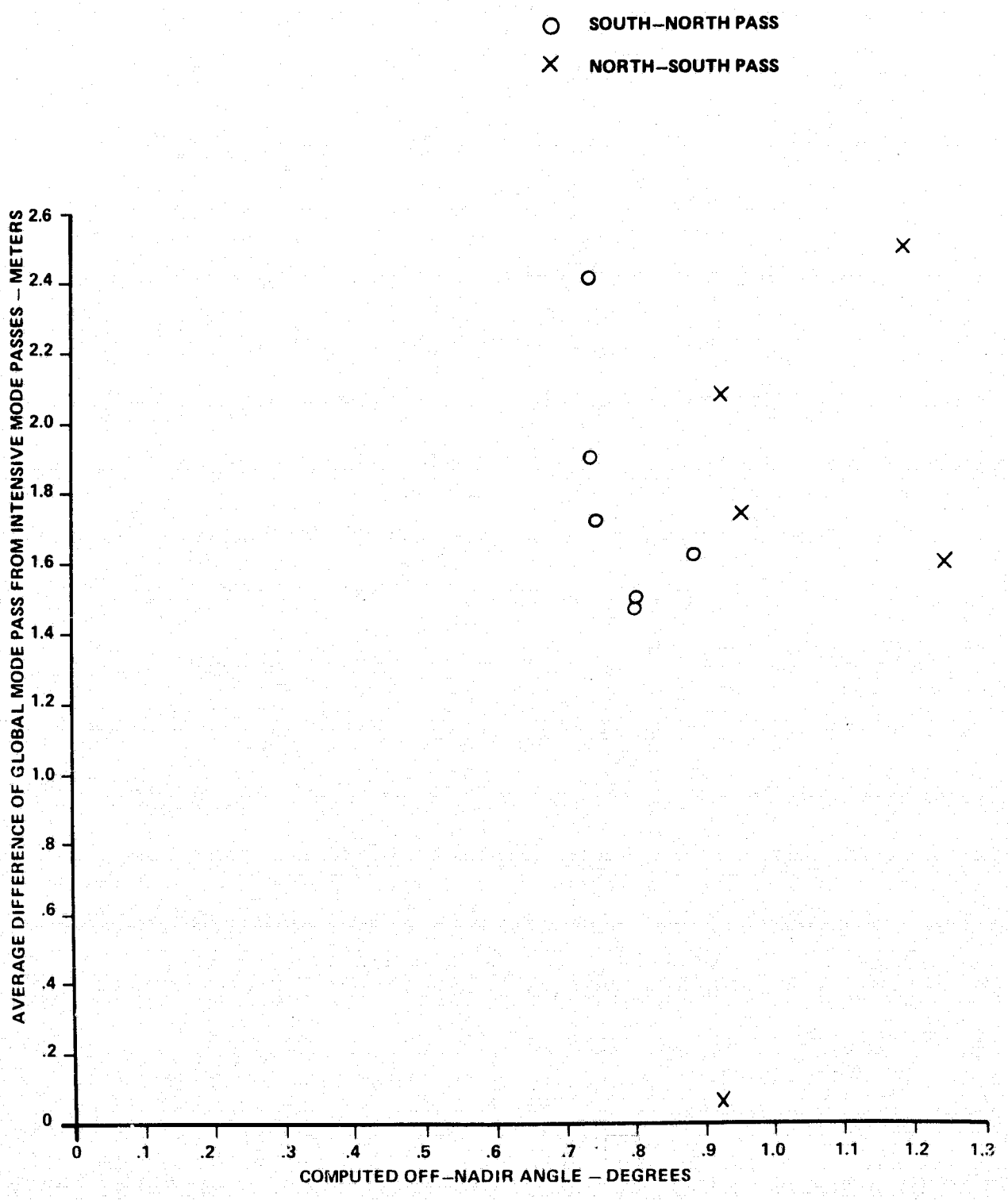

FIGURE 24. ESTIMATED GLOBAL MODE BIASES RELATIVE TO INTENSIVE MODE BIASES AS A FUNCTION OF COMPUTED OFF–NADIR ANGLE

orbit errors. Of the remaining two, only Rev 268 is of real concern. The most likely explanation is orbit error, in spite of the lack of visible evidence. The next most probably are sea state effects, and an actual pass to pass bias variation. As indicated above, Rev 410 suffers from probable orbit problems as well as apparent sea state effects in the vicinity of Bermuda.

We thus conclude that:

- Only one pass shows any suspicion of pass to pass bias variation, and other explanations are considered much more probable for the ~2 m deviation of this pass from the mean of the remaining consistent passes.

- There is no evidence of error in the algorithm used for computing the off-nadir effects on global mode altitudes, other than a possible bias which would be absorbed in the estimated global mode bias.

4.3 DATA NOISE LEVELS

As with the intensive mode data, the global mode passes were all smoothed, and the rss's of the raw measurements about the smoothed data calculated. Again, these numbers should closely approximate the measurement noise levels, although they may be slightly optimistic because of the 1 m a priori noise level assumed in the smoothing operation, whereas the actual noise level is somewhat higher. Figure 25 shows approximately 20 seconds of raw data for a rather typical (noise-wise) global mode pass, along with the smoothed altitudes obtained by ALTKAL.

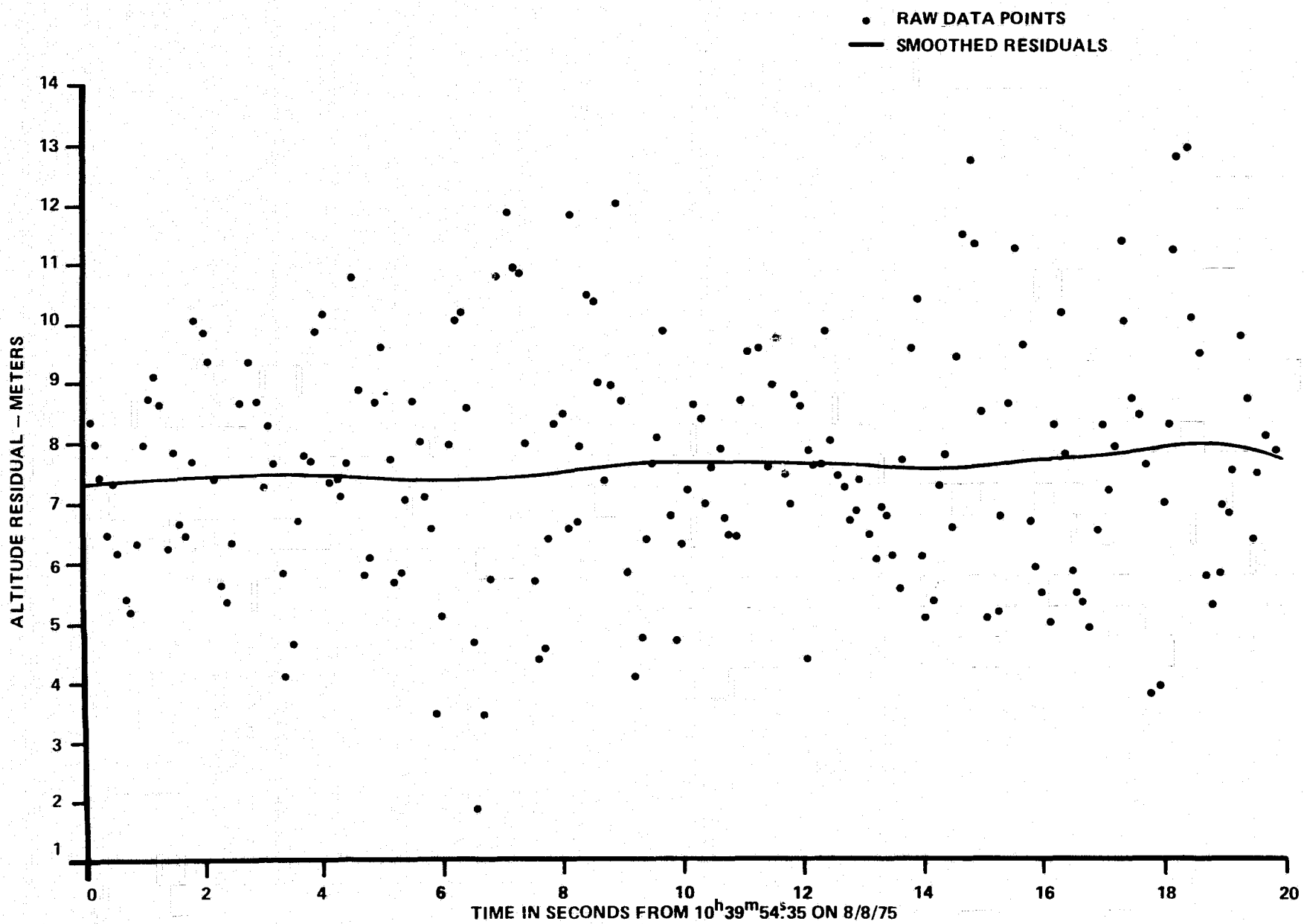

FIGURE 25. GLOBAL MODE CUMULATIVE ALTITUDES FOR A 20 SECOND SPAN OF REV 1704 SHOWING TYPICAL GLOBAL MODE NOISE LEVELS

Noise levels estimated for the 14 global mode passes are listed in Table 9. Similar to the intensive mode, 6-10 m anomalies are occasionally observed in the global mode data and have been edited in the smoothing operation. Such data points are not included in the rss computations. The overall rss for over 26000 points is 1.81 m, and there is no great spread of any pass about this value. The smallest rss is 1.59 m, and the largest is 1.93 m.

4.4 GLOBAL MODE BIAS ACCURACY ANALYSIS

The accuracy of the global mode bias can be assessed in several different ways, depending in part upon the method by which the bias is assumed to have been derived. One appealing method is as follows:

a. Assume the intensive mode bias to be pass to pass stable (as has been shown to be at least very nearly the case).

b. Assume the off-nadir correction procedure to be completely accurate, and no evidence of systematic error has been found.

c. Estimate the accuracy with which residuals from Revs 1178 and 1704 can be aligned for the complete calibration area pass.

d. Assume that the global mode bias is pass to pass stable. Again, the evidence to the contrary is quite weak.

Having made these assumptions, there are only three constituents in the global mode bias error:

Revolution	No. of Points	RSS (m)
254	2140	1.88
268	1607	1.70
274	1180	1.70
325	1979	1.96
331	1155	1.82
339	2160	1.91
345	1527	1.70
382	1926	1.93
402	1720	1.79
410	1755	1.92
1269	1333	1.78
1298	950	1.79
1312	1740	1.59
1582	1660	1.64
1696	1760	1.79
1704	2326	1.82
Total	26918	1.81

Table 9. Root sum of Squares of Raw Cumulative Global Mode Altitudes About Smoothed Altitudes

1. The intensive mode bias error.

2. The error in alignment of Revs 1704 and 1178.

3. The difference in the average orbital height error between Revs 1178 and 1704.

Of these three error sources, the first has been calculated to be 21 cm, the second does not exceed 20 cm, and the third is virtually negligible. The resulting sigma is about 30 cm.

Although the average bias listed in Table 8 was not derived from Rev 1704 alone, our bias estimate is the same as if we had and we will adopt a variation of the above argument for the bias accuracy assessment. We simply drop the assumption of the validity of the off-nadir model error and include an error component to account for its being only approximate. We then need only estimate a reasonable bound for the off-nadir model error.

Dropping Rev 268 as being unaccountably anomalous, the scatter in the remaining 11 entries in Table 8 is due to the combined total set of errors: measurement noise, station position errors, radar bias errors, varying propagation effects, as well as off-nadir model errors. Since the total rms of these 11 values in only 36 cm, the off-nadir component must be less than this, and we will adopt the pessimistic value of 30 cm. The resulting bias uncertainty, summarized in Table 10, is 42 cm. For errors at this magnitude, differences in propagation errors for Revs 1178 and 1704 have been neglected.

Unfortunately, comparison of the bias estimate obtained by G.E. [1] for the global mode does not show very close agreement with the Table 8 value. Again, based on the center-of-mass for a calibration reference, the respective values are:

Error Source	Magnitude of Assumed Error	Effect on Estimated Global Mode Bias
Intensive Mode Bias Error	21 cm	21 cm
Alignment of Revs 1178 and 1704	<20 cm	20 cm
Difference in Orbit Error between Revs 1704 and 1178	~0	~0
Error in Model for Correcting for Off-Nadir Pointing of GEOS-3 Altimeter Antenna	30 cm	30 cm
Total		42 cm

Table 10. Error Components for Global Mode Calibration

Table 8	1.75 - 5.27 = -3.52 m
G.E.	-0.68 m

The difference is almost 3 meters. Presumably, however, the G.E. number is for nadir pointing, and we have noted that the off-nadir model which we have used may be biased, thus inducing a corresponding effect on our bias estimate. This bias, however, cannot be less than -1.4 m, since this is the largest (algebraically) applied correction for off-nadir effects. This still leaves a discrepancy of at least 1.5 m unaccounted for.

SECTION 5.0
SUMMARY AND CONCLUSIONS

The altitude biases and noise levels that have been estimated for the GEOS-3 altimeter are summarized in Table 11. Also included is the timing bias that is calculated in Appendix A and which appears to be consistent with the data analysis results. The intensive mode bias was estimated using a TM Mode 2 pass. The consistency of the bias was validated using both TM Mode 1 and TM Mode 2 data. On the basis of a sample of 2, the TM Mode 3 data appears to be consistent with the G.E. calculation of a 47 cm difference between the bias in TM Mode 3 and TM Modes 1 and 2. For the 3 TM modes, there is reasonable ($\sim 1\sigma$) consistency between the Table 11 results and the G.E. bias estimates obtained from hardware analyses.

The global mode bias number is based upon the application of an off-nadir pointing correction, using average plateau and attitude-specular gate voltages. Although the model computes off-nadir angles which are suspected of being biased, the resulting altitude corrections do not show evidence of being off-nadir angle dependent. The correction model for off-nadir effects thus appears quite satisfactory for its intended application. Agreement of the estimated bias and the bias obtained by G.E. is not good, differing by about 3 m.

The calculated timing correction of -11.59 msec should be applied to the time tags of "last effective transmitted pulses," in the vernacular of the GEOS-C Preprocessing Report [18], and accounts for both STDN timing error and altimeter lag error. Time tags for smoothed altitudes on GEOS-3 data tapes have included a 1 msec lag correction and need a timing bias correction of -10.59 msec.

The average altimeter data noise levels listed in Table 11 are for cumulative altitudes, or ~10 pps data. These values

Altimeter Mode	Altitude Bias	Average Noise Level (10 pps data rate)	Calculated Timing Bias	
			Instantaneous Altitudes	Smoothed Altitudes
Intensive Mode Cumulative Altitudes (TM Formats 1 & 2)	-5.3m±.21m	72cm	-11.56msec	-10.56msec
Instantaneous Altitudes (TM Format 3)	-5.87m*	**		
Global Mode Cumulative Altitudes (TM Format 1)	-3.55m±.42m	1.81m		

*Based on TM Mode 2 calibration and G.E. calculation [1] of bias difference between instantaneous and cumulative altitudes.

**Not estimated, but no apparent difference from cumulative altitudes at same data rate.

Table 11. Summary of Estimated Altimeter Biases, Noise Levels, and Timing Errors. Negative Altitude Bias Means that Measurements are Short. Negative Timing Bias Means that Time Tags are too Long.

are based on 18 intensive mode passes and 16 global mode passes, and were computed from residuals about the smoothed altitudes produced by the ALTKAL data smoother.

Both the intensive and global modes exhibit anomalous periods in which the measurements are long by 6-10 m for about half a second. Although it has been observed through the intensive mode waveforms that the tracking (ramp) gate is misplaced in the return pulse, no real explanation was obtained for why the pulse became misplaced. When using the altitude data in smoothed form, such as from the ALTKAL smoother, these anomalies do not generally cause any real problem provided the anomalous points are edited.

A major conclusion that can be drawn from the calibration results is that there appear to be inherent limitations to the accuracy which can be achieved by the at-sea/geoid model calibration technique, due to the observed temporal sea surface height variations in large portions of the calibration area. For a single pass, the accuracy limitation is probably in the range of 10-30 cm due to the potential presence of eddies and other sea surface height variations not included in the tide model. And there is no assurance that averaging a number of passes would reduce the systematic effects of these (somewhat random) height changes. These limitations,of course, are in addition to the problems of obtaining an accurate geoid model, an accurate tide model, and accurate orbits.

The high elevation pass across Bermuda on GEOS-3 Rev 4553 must be considered fortuitous in that the groundtrack passed so close to the laser tracking station, which actually tracked on the pass. The procedure used in the bias estimation from this pass, however, is considered to be perfectly valid for any near-overhead pass of Bermuda, particularly in a South-North direction. If augmented with the use of tide

gauge measurements on Bermuda, the method appears to satisfactorily solve the geoid model problem and the temporal sea surface height problem. With these hurdles conquered, all other altimeter calibration problems should be minor.

APPENDIX A
Altimeter Data Time Tags

1. Altimeter Lag

Since the GEOS-3 altimeter tracking loop cannot respond instantaneously to a variation in the true altitude which should be measured, there will always be some "lag" in the output altitude. Knowledge of this lag is necessary to properly time tag the output altitudes. In general, the lag will be a function of:

1. The sea state within the altimeter footprint, since the tracking loop gain depends upon the slope of the return pulse leading edge.

2. Sea surface undulation features along the satellite groundtrack.

We will derive the proper altimeter time tag based upon two assumptions:

1. Low sea state (<2 m), which results in the nominal tracking loop gain.

2. A linear variation in sea surface height over the effective time for obtaining an output altitude.

Neither of these assumptions are believed to significantly affect the computed time tag. The derivation technique used below can, in fact, be used with other tracking loop parameters and any assumed variation of altitude with time.

Consider first the GEOS-3 tracking loop, a diagram of which is shown in Figure A-1, taken from p. 122 of the Altimeter Design Error Analysis Handbook [1]. The loop consists of a simple gain K_g, a loop filter with transfer function H_e, and an accumulator with gain K. The resulting open loop transfer function is then

$$A(z) = \frac{K_g \; K \; H_e(z)}{z-1} \tag{A-1}$$

$H_e(z)$ is given in Ref. 16, p. 124, as

$$H_e(z) = \frac{b}{a} \frac{z-1 + \frac{a}{b}(1-\beta)}{z-\beta} \tag{A-2}$$

with the constants given by [Ref. 16, p. 129],

$$\begin{aligned} a &= 7.792 \\ b &= 0.1275 \\ \beta &= \exp\,(-bT_s) = 0.9986951867 \\ T_s &= 0.010240512 \text{ seconds (sampling period)} \end{aligned} \tag{A-3}$$

The loop gain K_g K is based upon the altimeter design requirement that the lag error not exceed 1 ns. As a part of their system design to meet the lag requirement, G.E. chose the value of the velocity error coefficient to be

$$K_v \geq 1000/\text{sec.} \tag{A-4}$$

C-2

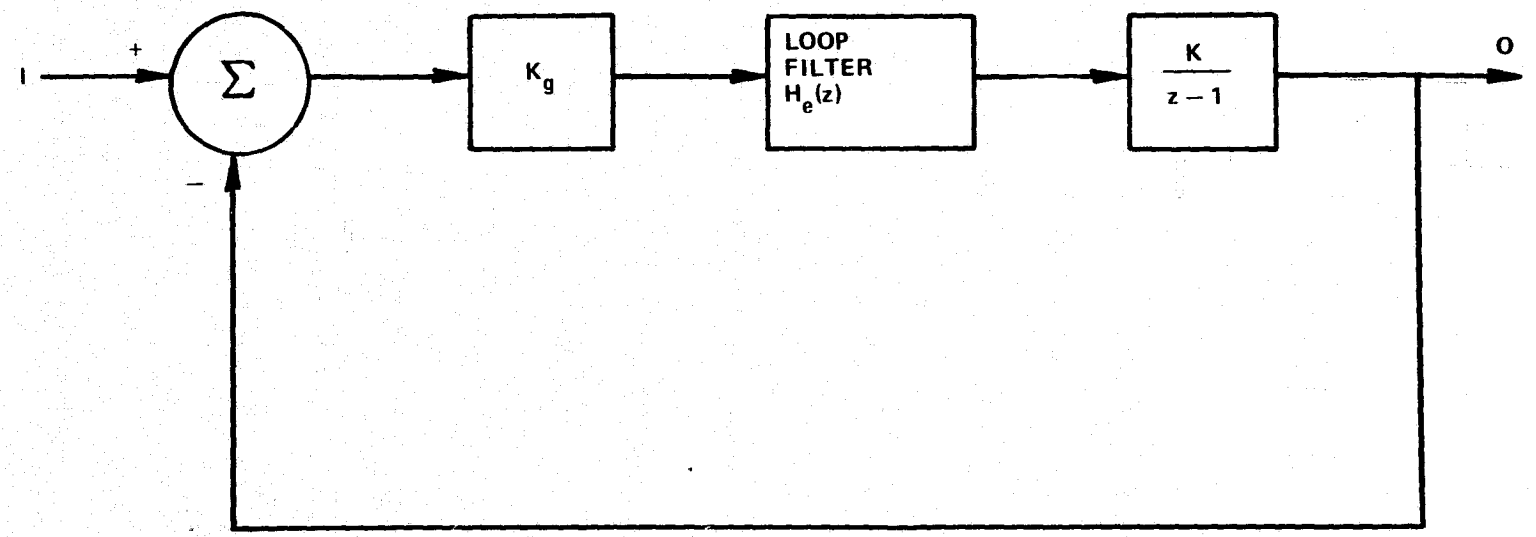

FIGURE A–1. EQUIVALENT LINEAR DISCRETE–TIME FEEDBACK LOOP MODEL FOR GEOS–3 ALTIMETER

For the chosen design, the loop gain is related to the velocity error coefficient as [Ref. 1, p. 125]

$$K_v = \frac{K_g K}{T_s} \tag{A-5}$$

Choosing the equal sign in Eqn. (A-4), the loop gain is then

$$K_g K = 1000 T_s = 10.240512 \tag{A-6}$$

Using Eqn. (A-1) for the open loop transfer function, the closed loop transfer function is given by

$$B(z) = \frac{A(z)}{1+A(z)} = \frac{b_1 z+b_2}{z^2+a_1 z+a_2} \tag{A-7}$$

where, from (A-3) and (A-6), the constants have the values

$$\begin{aligned} b_1 &= 0.167564846 \\ b_2 &= -0.15420289 \\ a_1 &= -1.831130341 \\ a_2 &= 0.8444922967 \end{aligned} \tag{A-8}$$

From (A-7), we can obtain the system output as a function of the input, since the Z transforms of the input I and output O are related by

$$O(z) = B(z)\ I(z) \tag{A-9}$$

To be able to readily obtain the inverse transforms, however, we need to express the closed loop transfer function as a power series in z^{-1}. That is, we set

$$B(z) = \sum_{k=0}^{\infty} b(k\ T_s)\ z^{-k} \tag{A-10}$$

The loop "weighting sequence", $b(k\ T_s)$, or simply $b(k)$, is found by comparing term by term the power series in z^{-1} in (A-10) with the equivalent series generated by long division of (A-7). The result is

$$\begin{aligned} b(0) &= 0 \\ b(1) &= b_1 \\ b(2) &= b_2 - a_1\ b_1 \end{aligned} \tag{A-11}$$

with the remaining coefficients given by the recursion relation

$$b(n) = -a_2\ b(n-2) - a_1\ b(n-1),\ n \geq 3. \tag{A-12}$$

Substituting (A-10) into (A-9),

$$O(z) = \sum_{k=0}^{\infty} b(k)\ z^{-k}\ I(z).$$

Taking inverse Z transforms of both sides, and considering that the system is causal with future input not influencing current output, we have

$$O(n) = \sum_{k=0}^{n} b(k)\ I(n-k) \qquad \text{(A-13)}$$

We are now ready to consider the form of the altitude input and deduce the appropriate time tag. By definition, the time tag for the output at time nT_s should equal the input at time qT_s

$$I(q) = O(n) \qquad \text{(A-14)}$$

and our objective is to determine n-q. Using our assumption No. 2, we will take the input altitude as having a linear time variation,

$$I(t) = \gamma t \qquad \text{(A-15)}$$

and thus

$$I(q) = \gamma q T_s \qquad \text{(A-16)}$$

Using the expression (A-13) for O(n),

$$I(q) = \sum_{k=0}^{n} b(k)\ I(n-k)$$

Substituting in this relation for I(q) and I(n-k) based on the ramp input, we obtain

$$\gamma q T_s = \sum_{k=0}^{n} b(k)\ \gamma\ (n-k)\ T_s \qquad \text{(A-17)}$$

from which

$$qT_s = nT_s \sum_{k=0}^{n} b(k) - \sum_{k=0}^{n} kT_s b(k) \qquad \text{(A-18)}$$

As n becomes very large, the summation

$$\lim_{n \to \infty} \sum_{k=0}^{n} b(k) \to 1,$$

or else a scale factor would be applied to the output altitudes. From Eqn. (A-18), we thus deduce the delay τ to be

$$\tau \equiv (q-n)\ T_s = -\sum_{k=0}^{\infty} k\ b(k)\ T_s \qquad \text{(A-19)}$$

Using Eqns. (A-8), (A-11) and (A-12) to obtain the coefficients b(k), we find that

$$\tau = -0.00100 \text{ seconds} \qquad \text{(A-20)}$$

The low order coefficients computed in the process of obtaining this delay are shown graphically in Figure A-2. Approximately 120 inputs are necessary in order for the final computed delay to converge to within 3%.

From Eqn. (A-11), and as shown in Figure 2, the weighting of the n^{th} input or the n^{th} output is zero. However, the output effectively lags less than a tenth of an interpulse period.

The above discussion has alluded only to a single altitude form of output, and is thus applicable to GEOS-3 "instantaneous" altitude measurements such as are obtained using Telemetry Mode 3. Figure A-2, in particular, shows the weighting of altitudes in an instantaneous altitude output. The more common telemetered altitudes are cumulative altitudes which are algebraic averages of ten instantaneous (individual) altitudes. An effective set of input data weights can be computed using those computed above. The resulting set of weights are shown in Figure A-3. Based on the linear time variation of altitude input, the appropriate time tag for the cumulative altitude is simply the time tag as computed above for the last instantaneous altitude used in the cumulative altitude, and then shifted 4.5 interpulse periods back in time to the middle of the 10 samples comprising the measurement.

The above weighting coefficients, although computed on the basis of a transfer function given in the G.E. Design Error Analysis Handbook, are not, strictly speaking, correct. In the set of weighting coefficients, there is one zero-weighted pulse. In fact, there should be two zero-weighted pulses, with a corresponding T_s + 1 msec lag rather than simply 1 msec. However, the existence of two unweighted pulses has been known since well before launch and has been included in the time tagging of all altimeter data processed at NASA/Wallops Flight Center. There is some complication, however, due to the extra pulse delay not being incorporated into the transfer function, with the result that the calculated delay is based upon a slightly incorrect transfer function which could give a slightly erroneous lag. It has been estimated by Hofmeister [19], however, that effects should be small, and we will here ignore them. Consistency of the actual data with the above lag estimates, as has been demonstrated for the intensive mode data, also confirms that the transfer function used is not significantly in error.

Figure A-2

WEIGHTING COEFFICIENTS FOR INSTANTANEOUS ALTITUDES

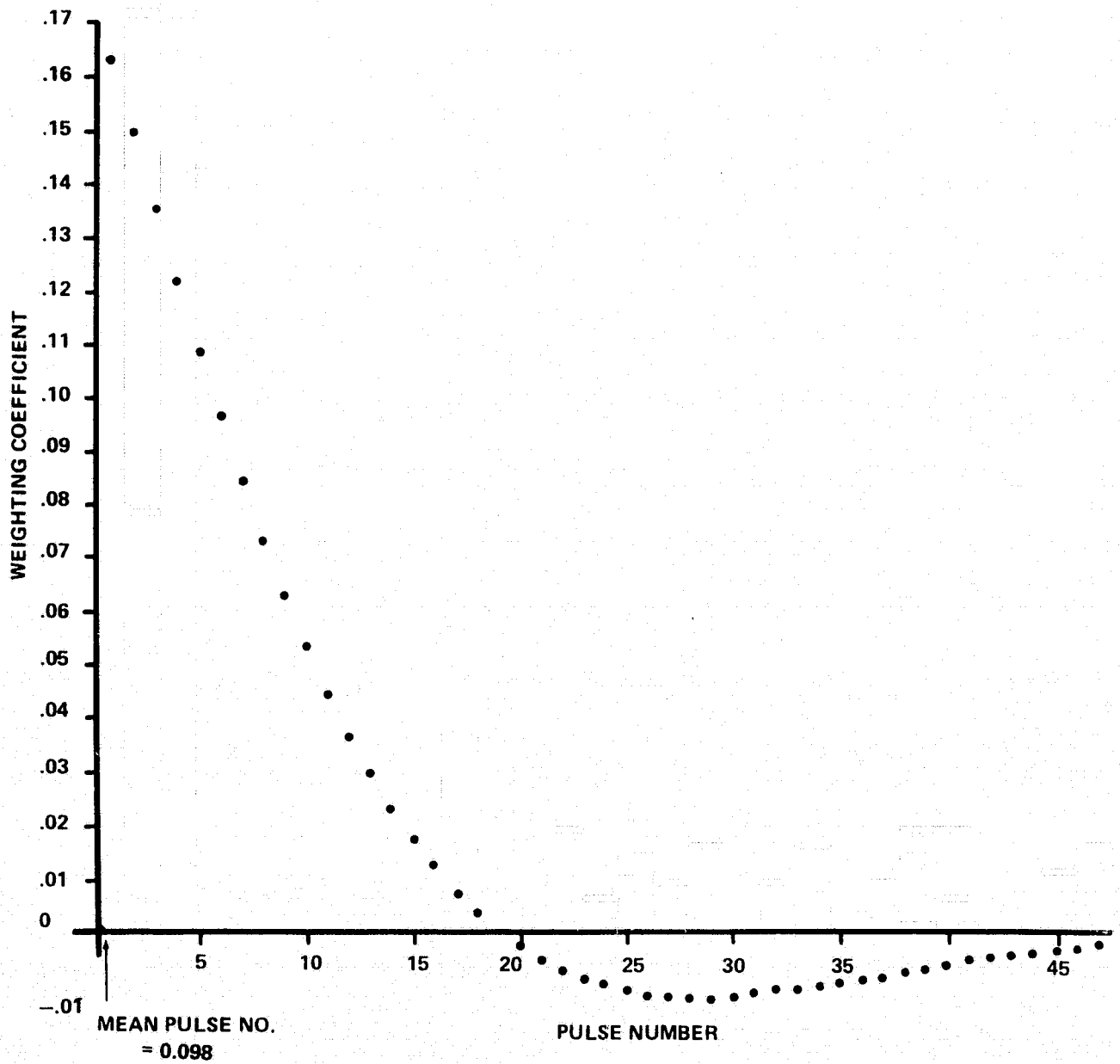

Figure A-3

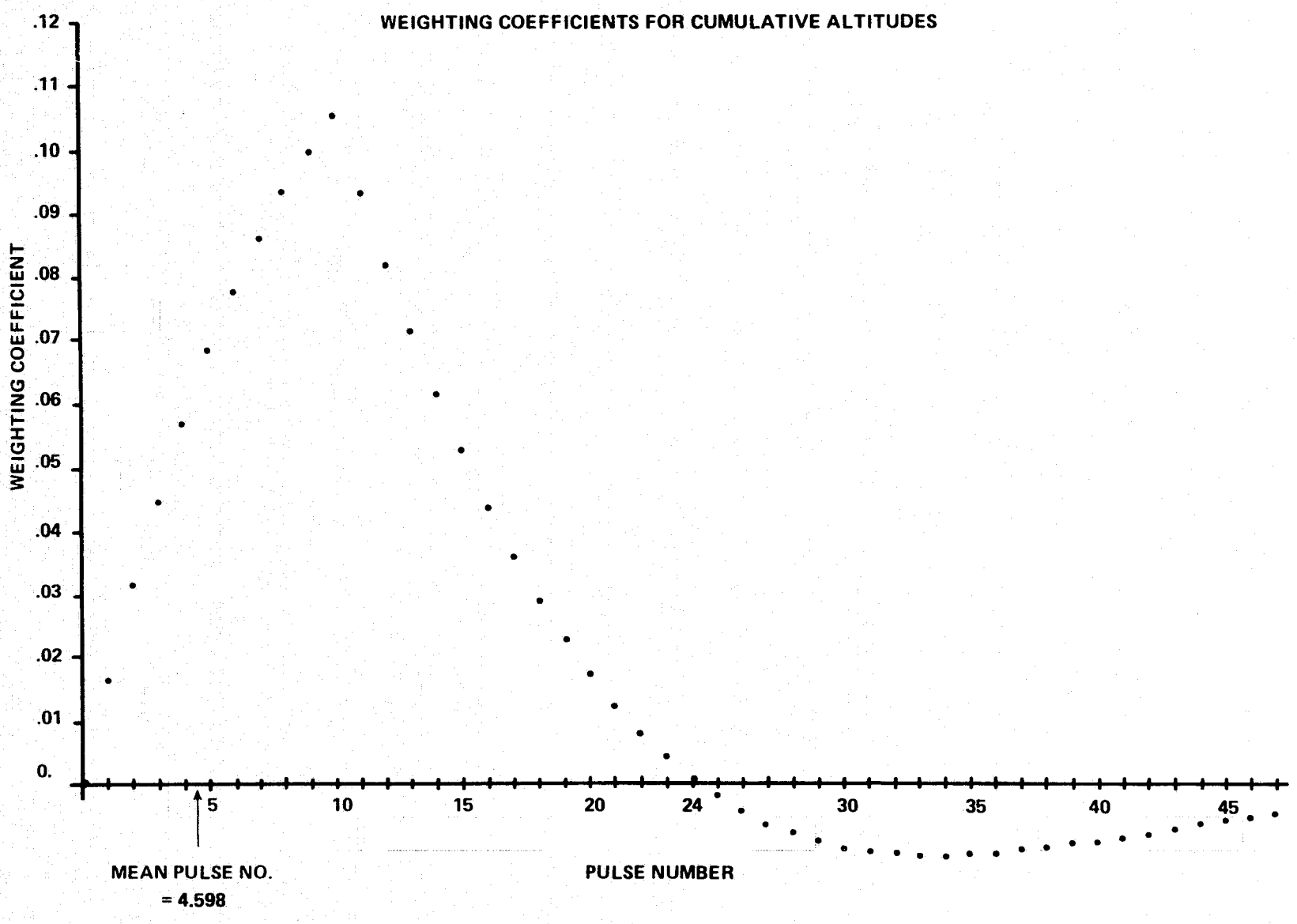
WEIGHTING COEFFICIENTS FOR CUMULATIVE ALTITUDES
WEIGHTING COEFFICIENT
.12
.11
.10
.09
.08
.07
.06
.05
.04
.03
.02
.01
0.
5
10
15
20
24
30
35
40
45
MEAN PULSE NO.
= 4.598
PULSE NUMBER

2. GEOS-3 Altimeter Data Timing

There are two time tags utilized on GEOS-3 altimeter data tapes. These are:

1. The time tag for the smoothed major frame average altitude, and the only altitude distributed on BCD tapes. This time tag should be fully corrected for transit time and the appropriate lags. This time tag is not presently correct, as will be discussed below.

2. Instantaneous and cumulative altitudes, only on the distributed binary tapes, which must be time tagged based upon a frame time and a Δt (different for instantaneous and cumulative altitudes) which produces a time defined as the time of the last effective transmitted pulse going into the sample of interest. In the context of the above discussion of weights, we should here consider "effective" as being synonomous with "weighted". With this interpretation, the time tagging of cumulative and instantaneous altitudes on distributed data should be considered correct, except for the STDN timing of GEOS-3 as discussed below.

Accordingly, we will discuss timing corrections that should be applied to smoothed altitudes on the one hand, and to instantaneous or cumulative altitudes on the other. We need to account for what "lag" corrections are presently made, what "lag" corrections should be made, and any known errors outside the altimeter and its data preprocessing. In the latter category is a STDN timing error for GEOS-3 which has been well substantiated [4] as being 20.8 msec, with the resulting time tags being too long. For smoothed

altitudes, the time tags on distributed data are, effectively, 1 msec earlier than the last weighted pulse in an instantaneous altitude [20]. For the instantaneous and cumulative altitudes, the shift of T_s - 1 msec forward should be made from the last weighted pulse. It may be noted that the result here will be a transmitted pulse time and that a transit time correction still needs to be applied. Furthermore, data users who feel like making lag corrections of their own should feel free to do so rather than using the numbers given below.

The corrections which should be applied to data processed and distributed from NASA/WFC are summarized in Table A-1. "Lag" numbers are referenced to the last weighted pulse, rather than the first unweighted pulse, to be consistent with terminology in the Altimeter Processing Report [18].

The STDN timing correction of -20.8 msec is strictly applicable to the time tags of all data telemetered from GEOS-3. Only altitudes, however, are likely to be significantly affected, and here the effect of the net ~11 msec error will be a maximum of about 30 cm in altitude. Especially after considering that the effects on altimeter cross-overs are of opposite sign (due to the altitude rates having opposite signs from North-South and South-North passes), the timing error is by no means negligible, particularly for intensive mode data.

Error Source	Correction	
	Smoothed Altitudes	Instantaneous and Cumulative Altitudes
STDN Timing	-20.8 msec	-20.8 msec
- Present Lag Correction	- (-1.0 msec)	None
+ Computed Lag Correction (T_s-1 msec)	+ 9.241 msec	+9.241 msec
Total Correction	-10.559 msec	-11.559 msec

Table A-1. Timing Corrections for GEOS-3 Altitude Time Tags

APPENDIX B
LASER STATION POSITION ESTIMATION

All the orbits used in Sections 3 and 4 for altimeter calibration were based on data from a single pass of GEOS-3 with tracking by calibration area stations. The passes which have been used in the altimeter crossover analysis have been those with tracking by lasers at Goddard, Bermuda, and Grand Turk. A total of 18 such passes exist with simultaneous altimeter data, as has been discussed in Section 3.2. If data from the Range Measurements Laboratory (RML) is included, 3 laser tracking exists for a number of other passes. The RML data will be discussed below.

In order to obtain positions for the 3 NASA lasers which would produce sufficiently precise orbits for the cross-over analysis, baselines between the stations and relative station heights had to be obtained as accurately as possible. Such positioning was attempted through the use of single pass arcs of GEOS-3 with 3 laser tracking, and with good balance between North-South and South-North passes. Since such solutions really have only baseline adjustment capability, one latitude and two longitudes were held fixed and only slight adjustment in heights were allowed. The a priori positions used were from an intermediate center-of-mass solution obtained by Marsh and Conrad [21] using predominantly GEOS-3 data. The orientation of the solution and, to a large degree the station heights are determined by the a priori positions used.

Table B-1 summarizes the results of the 14 arc solution used for estimating the NASA laser positions. The overall data fit is 7.4 cm rms, with generally only minimal data editing. The most anomalous pass is Rev 1576, with unusually high residual fit for Bermuda. No systematic editing of data

Table B-1. Data Used and RSS of Fit After Station Adjustment for 14 Laser Arcs

GEOS-3 Rev No.	Date	Approx. Time	STALAS		BERMUDA		GRAND TURK		PASS TOTAL	
			No. of Wtd. Pts.	RSS (cm)	No. of Wtd. Pts.	RSS (cm)	No. of Wtd. Pts.	RSS (cm)	No. of Wtd. Pts.	RSS (cm)
1178	7/2/75	06^h18^m	126	5.6	188	6.4	14	8.3	328	6.2
1576	7/20/75	09^h30^m	100	6.9	177	21.0	230	6.9	507	13.7
1710	8/8/75	20^h19^m	63	4.6	125	5.5	185	5.9	373	5.6
1718	8/9/75	10^h20^m	29	3.6	105	6.8	123	9.6	257	8.1
1974	8/27/75	12^h40^m	172	6.7	68	12.7	84	6.3	324	8.3
1980	8/27/75	22^h18^m	289	5.4	322	6.3	274	5.6	885	5.8
1988	8/28/75	12^h04^m	35	4.9	224	6.8	190	5.0	449	6.0
2094	9/4/75	23^h42^m	107	5.4	148	6.3	147	8.5	402	7.1
2102	9/5/75	13^h46^m	89	8.9	296	5.8	161	12.3	546	8.8
2151	9/9/75	00^h22^m	294	5.6	241	5.9	100	8.1	635	6.2
4519	2/23/76	10^h00^m	121	6.0	43	4.7	68	4.2	252	5.4
4553	2/25/76	19^h09^m	2	0.8	33	5.1	145	5.0	180	5.1
4610	2/29/76	19^h50^m	76	5.6	161	9.0	225	4.0	462	6.4
4624	3/1/76	19^h38^m	37	4.9	284	5.0	100	5.0	421	5.0
								Total	6021	7.4

on this pass, however, would appear to significantly improve the fit, and the pass was retained in its entirety. The only other passes with residual fits greater than 10 cm were Bermuda on Rev 1974 and Grand Turk on Rev 2102. Many passes have fits in the 5 cm region.

The station positions estimated in the 14 arc solution are listed in Table B-2, and the corresponding baselines are listed in Table B-3. Baseline accuracies are estimated to be in the 10-20 cm region, with 25 cm probably an upper bound.

Since there are several altimeter passes which have 4 laser tracking, an attempt was made to estimate the position of the RML laser (RAMLAS) in order to obtain the best possible orbits for these passes. It was found, however, that the RAMLAS data for the time periods of interest had timing problems at about the 0.5 msec level. Several solutions were made in which the position of RAMLAS and its timing errors were estimated along with the positions of the 3 NASA lasers. Tables B-4 - B-6 give the results of one such solution which included 19 arcs (the 14 arcs discussed above, with RAMLAS data added to Rev 4610, and 5 additional arcs) with an adjustment for both a range and timing bias for each RAMLAS pass. Table B-4 lists the station positions adjusted, Table B-5 gives the corresponding baselines, and Table B-6 lists the estimated range biases and timing biases for RAMLAS.

Baselines for the Goddard lasers listed in Table B-5 differ by 9, 4, and 6 cm from those listed in Table B-3. Since the solution with RAMLAS also includes 6 bias and 6 timing bias parameters, this agreement should probably not be surprising and really does not serve to significantly validate the accuracy of either solution, although it does tend to validate the added NASA laser data.

Name	Number	Latitude	Longitude	Spheroid Height*
STALAS	7063	39°01'13".544	283°10'19".751	16.195 m
BDALAS	7067	32°21'13".967	295°20'37".918	-25.904 m
GRTLAS	7068	21°27'37".989	288°52'05".004	-21.636 m

*Referenced to an ellipsoid with a_e = 6378145 m, f = 1/298.255

Table B-2. Estimated Station Positions from 14 Arc Laser Solution
Latitude for STALAS and Longitudes for STALAS and GRTLAS not Estimated

Stations	Baseline Value (m)
STA - BDA (7063 - 7067)	1322742.01
STA - GRT (7063 - 7068)	2012724.66
BDA - GRT (7067 - 7068)	1364265.16

Table B-3. Baselines for Station Positions Estimated from 14 Arc Laser Solutions

The RAMLAS parameter recoveries summarized in Table B-6 show amazingly consistent timing biases throughout the month of February 1976 and apparently a significantly different timing bias in December 1975. The range bias recoveries are also surprising in their consistency, with one pass apparently a significant outlier. The range bias recoveries are all the more amazing in that they appear to be in rather close agreement with the results obtained by Berbert [22] in the collocation tests at Patrick AFB in April 1976. At this time, however, any timing error on the order of 500 μsec had disappeared.

Several test orbits using the RAMLAS data and the station position solution given in Table B-4 indicated that crossover differences were affected at the sub-10 cm level.

Name	Number	Latitude	Longitude	Spheroid Height
STALAS	7063	39°01'13".568	283°10'19".751	16.91 m
BDALAS	7067	32°21'14".017	295°20'27".941	-24.87 m
GRTLAS	7068	21°27'38".031	288°52'5".051	-20.82 m
RAMLAS	7069	28°13'40".859	279°23'39".327	-25.83 m

Table B-4. Estimated Station Positions from 19 Arc Solution Including 6 Arcs with RAMLAS. Latitude for STALAS and Longitudes for STALAS and GRTLAS were not Adjusted.

Stations	Baseline Value (meters)
STA - BDA (7063 - 7067)	1322742.10
STA - GRT (7063 - 7068)	2012724.70
BDA - GRT (7067 - 7068)	1364265.22
STA - RAM (7063 - 7069)	1244991.23
BDA - RAM (7067 - 7069)	1213393.42
GRT - RAM (7068 - 7069)	1595083.25

Table B-5. Baselines for Estimated Station Positions from 19 Arc Laser Solution Including 6 Arcs with RML Laser Data

GEOS-3 Rev No.	(Dir.)	Date	Bias Recoveries Range Bias(cm)	Timing Bias(μsec)
3566	(N-S)	12/18/75	8.41 ± 9.54	358.9 ± 61.4
4340	(S-N)	2/10/76	63.29 ± 9.76	523.6 ± 37.2
4391	(N-S)	2/14/76	17.10 ± 6.58	549.5 ± 33.5
4482	(S-N)	2/20/76	24.41 ± 18.98	529.6 ± 39.0
4604	(N-S)	2/29/76	12.26 ± 8.48	550.8 ± 32.9
4610	(S-N)	2/29/76	24.64 ± 17.54	513.2 ± 35.0
			Wt. Av. of all except Rev 4340 = 14.92 ± 4.3	Wt. Av. of Feb. 1976 passes = 534.5 ± 15.8

Table B-6. Bias Parameter Recoveries for RAMLAS from 19 Arc Laser Solution. Sigmas Listed Include only Measurement Noise of 10 cm for all Stations.

APPENDIX C
BERMUDA TIDE HEIGHTS FOR REV 4553

The overhead calibration results of Section 3.1.2 are critically dependent upon the tidal correction applied to sea surface heights in the vicinity of Bermuda. The Mofjeld [8] model calculates a tide height of +12 cm for the geographic position of Bermuda at the time of the Rev 4553 pass. The tide model, however, was never proposed as being valid around islands, so any relation between 12 cm and the true tide at Bermuda at this time is almost accidental.

There are, however, two tide stations on the island of Bermuda, the locations of which are shown on Figure C-1. The Rev 4553 groundtrack is also shown on this figure. Figure C-2 shows the tide predictions [16] for the two tide stations, with interpolations between the predicted heights for the Ferry Reach tide station, the station closest to the altimeter groundtrack. At the time of the Rev 4553 pass, interpolation for the Ferry Reach station gives a tide height of 0.15 ft., or about 5 cm. Accepting this value, the applied tidal correction from the Mofjeld model is too large by about 7 cm, as is summarized in Table C-1.

In the overhead calibration, it should be noted that no weight was given to altimeter data for which land was contained in the footprint. Since the footprint diameter is about 5 km, the subsatellite point will not be closer than 2.5 km (~1.4') for any data utilized for the Rev 4553 pass. On the north side of the island for this pass, the water depths are on the order of 15 m for an extended distance from land and the tide gauge readings should give a reliable estimate of tide heights. However, on the south side of the island, the footprint for the last data point used before the altimeter

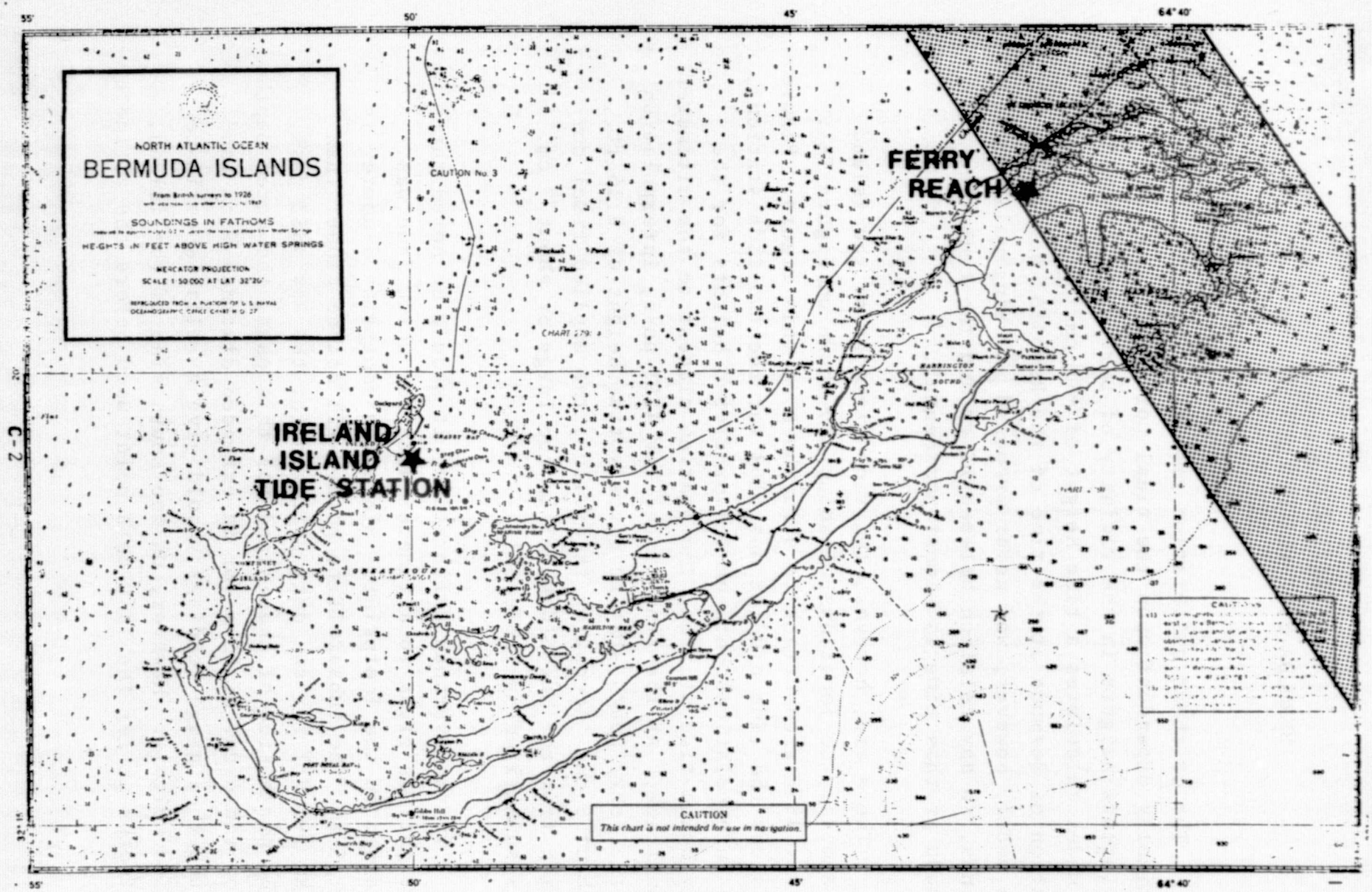

FIGURE C–1. ISLAND OF BERMUDA SHOWING LOCATION OF TIDE STATIONS AND APPROXIMATE FOOTPRINT FOR GEOS–3 REV 4553 PASS

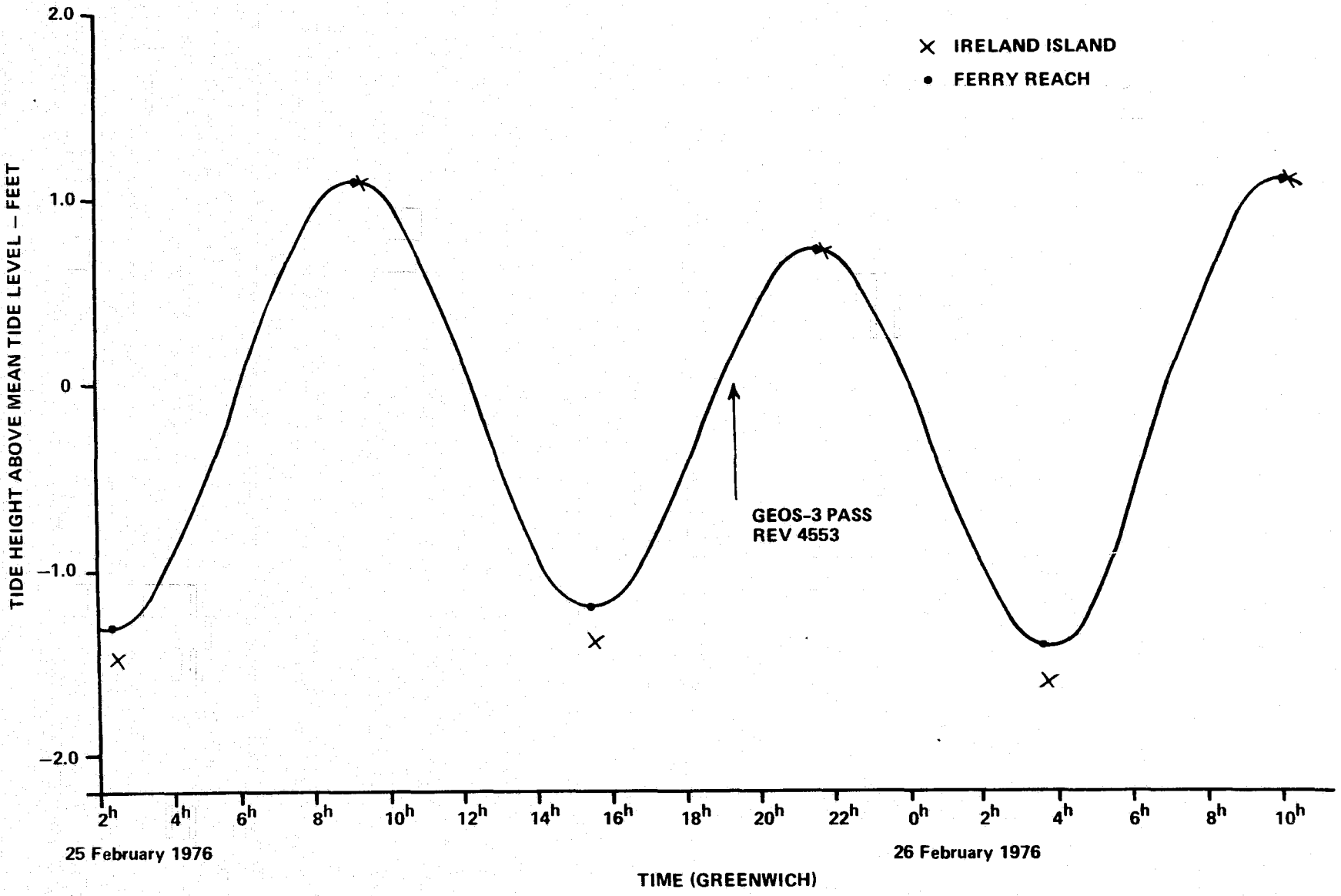

FIGURE C–2. BERMUDA TIDE HEIGHTS AROUND THE TIME OF THE REV 4553 PASS

Tide Height from Ferry Reach Tide Station	+ 5 cm
- Tide Height Applied (Mofjeld Deep Sea Model)	-(+ 12 cm)
Net Tide Correction	- 7 cm

Table C-1. Tide Correction to Altimeter Data Across Bermuda

started across the island included ocean depths ranging from about 10 m to almost a km. Earlier data points, which would also have had extensive weight in the interpolated altimeter points across land, would have been for deeper water for which the deep sea tide model should be nearly valid. Particularly since the laser site is near the south side of the island, the net result is that the effective tide effect on the interpolated data across the laser site should be somewhere between the deep sea tide value and the tide gauge values. Having no valid means of interpolating between the two values, except that the tide gauge values should be given full weight on the north side of the island and some weight on the south side, we have adopted the tide gauge tide height. We would expect that the error incurred is in the direction of underestimating the tide height, probably by on the order of 3 cm.

REFERENCES

1. Hofmeister, E.L., B.N. Keeney, T.W. Godbey, and R.J. Berg, "Data User's Handbook and Design Error Analysis - GEOS-3 RADAR ALTIMETER," Vol. I, General Electric Company Report, prepared for NASA/Wallops Flight Center and The Johns Hopkins University/Applied Physics Laboratory, May 1976. An early edition of the Design Error Analysis was published in May 1975.

2. Martin, C.F., and M.L. Butler, "GEOS-3 Calibration Results for the First Month of Operation," prepared under Contract NAS 6-2639 for NASA/Wallops Flight Center, Wallops Island, Virginia, January 6, 1976.

3. Marsh, J.G., and S.A. Vincent, "Geoid Computation and Analysis for the GEOS-C Altimeter Calibration Area," GSFC Report prepared for NASA/WFC, 1 August 1975.

4. Dwyer, R.W., Private Communication.

5. Martin, T.V., et.al., "GEODYN System Description," prepared by EG&G/WASC for NASA/Goddard Space Flight Center under Contract NAS 5-22849, August 1976.

6. "Mathematical Description of the ORAN Error Analysis Program," Wolf Research and Development Corporation, Planetary Sciences Department Report No. 010-73, September 1973.

7. Marsh, J.G., and E.S. Chang, "5' Detailed Gravimetric Geoid in the Northwestern Atlantic Ocean," Marine Geodesy, to be published.

8. Mofjeld, H.O., "Empirical Model for Tides in the Western North Atlantic Ocean," NOAA Technical Report ERL 340-AOML-19, October 1975.

REFERENCES
(Cont.)

9. Coriell, K.P., Geodynamics Experimental Ocean Satellite-3 Post Launch Attitude Determination and Control Performance, CSC Report No. TM-75/6149, prepared for NASA/GSFC under Contract NAS 5-11999, August 1975.

10. Miller, L.S. and G.S. Borwn, "Engineering Studies Related to the GEOS-C Radar Altimeter, Final Report for Task D," Applied Science Associates, Inc., Apex, N.C., May 1974, prepared under Contract NAS 6-2307 for NASA/Wallops Flight Center, Wallops Island, Va.

11. Hayne, G.S., L.S. Miller, and G.S. Brown, "Studies Related to Ocean Dynamics, Final Report for Task 3.1: Altimeter Waveform Software Design," Applied Science Associates, Inc., Apex, N.C., April 1975, prepared under Contract NAS 6-2520 for NASA/Wallops Flight Center, Wallops Island, Va.

12. Brown, G.S., "Global Mode Altitude Bias as a Function of Pointing Angle and Pointing Angle Estimation," Applied Sciences Associates, Inc., Apex, N.C., 23 September 1975, Memorandum to H.R. Stanley, NASA/Wallops Flight Center.

13. Goodman, L. "GEOS-C Ground Truth Program Description Document," NASA/Wallops Flight Center, March 1975.

14. Martin, C.F., "Altimeter Error Sources at the 10 cm Performance Level," prepared under Contract NAS 6-2639 for NASA/Wallops Flight Center, Wallops Island, Va., August 2, 1976.

15. Fang, B.T., "An Optimum Linear Filter for GEOS-3 Altimeter Data," prepared under Contract NAS 6-2639 for NASA/Wallops Flight Center, Wallops Island, Va., December 1976.

REFERENCES
(Cont.)

16. "Tide Tables 1976, High and Low Water Predictions, East Coast of North and South America including Greenland," National Oceanic and Atmospheric Administration, National Ocean Survey, Issued 1975.

17. Hofmeister, E.L., and B.N. Keeney, Private Communication.

18. Leitao, C.D., C.L. Purdy, and R.L. Brooks, "Wallops GEOS-C Altimeter Preprocessing Report," NASA/Wallops Flight Center Technical Memorandum No. NASA TM-X-69357, May 1975.

19. Hofmeister, E.L., Private Communication, January 1977.

20. Martin, C.F., "Smoothed Altimeter Data Timing," Memo to GEOS-3 Project Scientist, 4 September 1975.

21. Marsh, J.G. and T.D. Conrad, Private Communication.

22. Berbert, J.G., Private Communication.